UNIVERSITY OF CALIFORNIA, SAN DIEGO

p105 and p100 proteins function as the core of heterogeneous NF-kappaB complexes

A dissertation submitted in partial satisfaction of the

requirements for the degree Doctor of Philosophy

in

Chemistry

by

Olga V. Savinova

Committee in charge:
Professor Gourisankar Ghosh, Chair
Professor Robert Continetti
Professor Daniel Donoghue
Professor Christopher Glass
Professor Alexander Hoffmann
Professor Joseph Noel
Professor Susan Taylor

2009

The Dissertation of Olga V. Savinova is approved, and it is acceptable in quality and form for publication on microfilm and electronically:

_____

_____

_____

_____

_____

_____

_____

Chair

UNIVERSITY OF CALIFORNIA, SAN DIEGO

2009

Table of contents

List of Abbreviations

ANK	ankyrin repeats domain
ATCC	American Type Culture Collection
BMDM	bone marrow derived magrophages
cDNA	coding DNA
CE	cytoplasmic extract
CTD	carboxy-terminal domain
DLS	dynamic light scattering
DOC	deoxycholate, sodium salt
FLAG	peptide with sequence Asp-Tyr-Lys-Asp-Asp-Asp-Asp-Lys
GF	gel filtration
GFP	green fluorescent protein
GRR	glycin rich region
GST	glutathione S-transferase
IκB	inhibitor of NF-κB
IKK	inhibitor of NF-κB kinase
IP	immunoprecipitation
kD	kiloDalton
LPS	lipopolysaccharide
LTβ	lymphotoxin beta
LTβR	lymphotoxin beta receptor
MC	multinomial coefficient
MEF	mouse embryonic fibroblast
MW	molecular weight

NE	nuclear extract
NEMO	NF-κB essential modulator
NIK	NF-κB inducing kinase
NF-κB	nuclear factor kappa B
NLS	nuclear localization sequence
PAGE	polyacrylamide gel electrophoresis
PMA	phorbol 12-myristate 13-acetate
RHD	Rel homology domain
SDS	sodium dodecyl sulfate
SLS	static light scattering
TEV	tobacco etch virus
TLR	Toll-like receptor
WB	western blotting
YFP	yellow fluorescent protein

List or Figures

List of Tables

Acknowledgments

I would like to thank my advisor, Gourisankar Ghosh, for the opportunity to work on p105 and p100 project that led to the discovery of high molecular weight NF-κB complexes. I would also like to thank Alexander Hoffmann, Alexei Savinov, and Souman Basak for their valuable input in this project in the form of the scientific discussions, experimental advice and the reagents. I thank Bruce Worcester for his critical reading of our manuscript in preparation for publication, "p105 and p100 NF-κB precursors function as a core of multi-protein heterogeneous NF-κBsomes", which was instrumental to improve the clarity of my writing.

I would like to thank UCSD professors Lynn ten Eyck for teaching Macromolecular Modeling course, Philip Bourne for Structural Bioinformatics course, Stanley Opella for Protein NMR course, and Timothy Baker for TEM course. I joined the Ph.D program at the Department of Chemistry and Biochemistry with the goal to learn the structural aspects of molecular function. I am fortunate that my expectations were amply satisfied by educational opportunities these courses provided. I thank all UCSD and visiting scientists I was fortunate to interact with and learn from for their positive influence on my education and research.

This research was supported by NIH grant (A1064326) to GG, and by American Heart Association pre-doctoral fellowship (0715041Y) to OVS. I would also like to acknowledge the Biophysics Training Grant and the Keystone Symposia for travel assistance that allowed me to participate in the Gordon Research Conference on Proteins (2005) and in the Keystone Symposia on NF-κB (2008).

Chapters 2 and Chapter 3 have been submitted for publication of the material as it may appear in Molecular Cell, 2009. Savinova, Olga V.; Ghosh, Gourisankar. "p105 and p100 NF-κB precursors function as a core of multi-protein heterogeneous NF-κBsomes". The dissertation author was the primary investigator and author of this paper.

Figures 4.1, 4.2, and 4.3A in Chapter 4 are reprinted with permission as it appears in EMBO Journal, 2006. Moorthy, Anu K.; Savinova, Olga V.; Ho, Jessica Q.; Wang, Vivien Y-F.; Vu, Don; Ghosh, Gourisankar. "The 20S proteasome processes NF-κB1 p105 into p50 in a translation independent manner". EMBO; 25(9):1945-56; 2006. The dissertation author was the co-author on this paper.

Vita

Professional Employment:

2002-2003	Research specialist
	Howard Hughes Medical Institute
	The Jackson Laboratory, Bar Harbor, ME
1996-2002	Professional Research assistant
	The Jackson Laboratory, Bar Harbor, ME
1994-1996	Research assistant
	University of Maryland Biotechnology Institute, Baltimore, MD
1992-1994	Junior researcher
	Institute for Experimental Medicine, St. Petersburg, Russia

Qualifications:

2009	Ph.D. in Chemistry
	University of California, San Diego

Dissertation: “p105 and p100 proteins function as the core of heterogeneous NF-κB complexes”

1994	M.S. in Biochemistry
	St. Petersburg State University, St. Petersburg, Russia

Thesis: “The role for oxidized low density lipoproteins in the development of atherosclerosis”

Awards:

2008	Keystone Symposia Scholarship, NF-κB meeting

Short talk: “Molecular Organization of Endogenous p105 and p100 Complexes and their Role in LPS Signaling”

2007-2008 American Heart Association pre-doctoral fellowship

Funded proposal: “Structural determinants of p100 processing”

Publications:

1. Shih VF, Kearns DJ, Basak S, Savinova OV, Ghosh G, Hoffmann A. Kinetic control of negative feedback regulators determines their stimulus-specific functions within the NF-κB signaling system. 2008 (in revision, PNAS)

2. Savinova OV, Ghosh G. p105 and p100 NF-κB precursors function as a core of multi-protein heterogeneous NF-κBsomes 2008 (in revision, Mol. Cell)

3. Fusco AJ, Savinova OV, Talwar R, Kearns JD, Hoffmann A, Ghosh G. Stabilization of RelB requires multidomain interactions with p100/p52. J Biol Chem. 2008 May 2;283(18):12324-32

4. Gould DB, Marchant JK, Savinova OV, Smith RS, John SW. Col4a1 mutation causes endoplasmic reticulum stress and genetically modifiable ocular dysgenesis. Hum Mol Genet.; 2007 Apr 1;16(7):798-807.

5. Moorthy AK, Savinova OV, Ho JQ, Wang VY-F, Vu D, Ghosh G. The 20S proteasome processes NF-κB1 p105 into p50 in a translation independent manner. EMBO; 25(9):1945-56; 2006

6. Libby RT, Anderson MG, Pang I-H, Robinson Z, Savinova OV, Cosma IM, Snow A, Wilson LA, Smith RS, Clark AF and John SWM. Inherited glaucoma in DBA/2J mice: pertinent disease features for studying the neurodegeneration. Vis Neurosci.; 22(5):637-48; 2005

7. Libby RT, Li Y, Savinova OV, Barter J, Smith RS, Nickells RW, John SW. Susceptibility to neurodegeneration in a glaucoma is modified by Bax gene dosage. PLoS Genet.; 1(1):17-26; 2005

8. Gould DB, Miceli-Libby L, Savinova OV, Torrado M, Tomarev SI, Smith RS, John SW. Genetically increasing Myoc expression supports a necessary pathologic role of abnormal proteins in glaucoma. Mol Cell Biol.; 24(20):9019-25; 2004

9. Mo JS, Anderson MG, Gregory M, Smith RS, Savinova OV, Serreze DV, Ksander BR, Streilein JW, John SW. By altering ocular immune privilege, bone marrow-derived cells pathogenically contribute to DBA/2J pigmentary glaucoma. J Exp Med.; 197(10):1335-44; 2003

10. Libby RT, Smith RS, Savinova OV, Zabaleta A, Martin JE, Gonzales FJ, John SW. Modification of ocular defects in mouse developmental glaucoma models by tyrosinase. Science; 299(5612):1578-81; 2003

11. John SWM, Savinova OV. Intraocular pressure measurement in mice: technical aspects. In: Systematic Evaluation of the Mouse Eye. Ed. Smith RS; CRS Press; 2002

12. Chang B, Smith RS, Peters M, Savinova OV, Hawes NL, Zabaleta A, Nusinowitz S, Martin JE, Davisson ML, Cepko CL, Hogan BL, John SW. Haploinsufficient Bmp4 ocular phenotypes include anterior segment dysgenesis with elevated intraocular pressure. BMC Genet.; 2(1):18; 2001

13. Kim BS, Savinova OV, Reedy MV, Martin J, Lun Y, Gan L, Smith RS, Tomarev SI, John SW, Johnson RL. Targeted Disruption of the Myocilin Gene (Myoc) Suggests that Human Glaucoma-Causing Mutations Are Gain of Function. Mol Cell Biol.; 21(22):7707-13; 2001

14. Savinova OV, Sugiyama F, Martin JE, Tomarev SI, Paigen BJ, Smith RS, John SW. Intraocular pressure in genetically distinct mice: an update and strain survey. BMC Genet.; 2(1):12; 2001.

15. Smith RS, Zabaleta A, Savinova OV, John SW. The mouse anterior chamber angle and trabecular meshwork develop without cell death. BMC Dev Biol.; 1(1):3; 2001

16. Anderson MG, Smith RS, Savinova OV, Hawes NL, Chang B, Zabaleta A, Wilpan R, Heckenlively JR, Davisson M, John SW. Genetic modification of glaucoma associated phenotypes between AKXD-28/Ty and DBA/2J mice. BMC Genet.; 2(1):1; 2001

17. Smith RS, Zabaleta A, Kume T, Savinova OV, Kidson SH, Martin JE, Nishimura DY, Alward WL, Hogan BL, John SW. Haploinsufficiency of the transcription factors FOXC1 and FOXC2 results in aberrant ocular development. Hum Mol Genet.; 9(7):1021-32; 2000

18. Savinova O, Joshi B, Jagus R. Abnormal levels and minimal activity of the dsRNA-activated protein kinase, PKR, in breast carcinoma cells. Int J Biochem Cell Biol.; 31(1):175-89; 1999

19. Chang B, Smith RS, Hawes NL, Anderson MG, Zabaleta A, Savinova O, RoderickH, Heckenlively JR, Davisson MT, John SW. Interacting loci cause severe iris atrophy and glaucoma in DBA/2J mice. Nat Genet.; 21(4):405-9; 1999

20. John SW, Smith RS, Savinova OV, Hawes NL, Chang B, Turnbull D, Davisson M, Roderick TH, Heckenlively JR. Essential iris atrophy, pigment dispersion, and glaucoma in DBA/2J mice. Invest Ophthalmol Vis Sci.; 39(6):951-62; 1998

21. Savinova OV, Matsukawa N, Smithies O, John SW. Mouse natriuretic peptide receptor 3 gene maps to proximal chromosome 15. Mamm Genome.; 8(10):788; 1997

22. Savinova O, Jagus R. Use of vertical slab isoelectric focusing and immunoblotting to evaluate steady-state phosphorylation of eIF2 alpha in cultured cells. Methods In Enzymology.; 11(4):419-25; 1997

23. Swaminathan S, Rajan P, Savinova O, Jagus R, Thimmapaya B. Simian virus 40 large-T bypasses the translational block imposed by the phosphorylation of elF-2 alpha. Virology.; 219(1):321-3; 1996

24. Kuryshev VIu, Drapchinskaia NL, Tsarapkina EV, Savinova OV, Vorob'ev EV, Dizhe EB, Denisenko AD, Perevozchikov AP. Effective expression of the apolipoprotein A-I gene,

transferred to growing human cells in vitro Biull Eksp Biol Med.; 118(11):479-82. (Russian); 1994

ABSTRACT OF THE DISSERTATION

p105 and p100 proteins function as the core of heterogeneous NF-kappaB complexes

by

Olga V. Savinova

Doctor of Philosophy in Chemistry

University of California, San Diego, 2009

Professor Gourisankar Ghosh, Chair

Biochemistry of the components of signal transduction pathways provides a foundation for the understanding of how cellular signaling events initiate, propagate, and terminate. This thesis describes the multi-protein heterogeneous complexes of NF-κB with p105 and p100 proteins. Chapter 1 introduces the NF-κB signaling pathway and provides the rational for this thesis research. Chapter 2 describes the results of biochemical characterization of endogenous NF-κB and IκB proteins that led to the discovery of the high molecular weight heterogeneous complexes of p105 and p100 with other NF-κB subunits. Our results show that p105 and p100 complexes function to dynamically sequester newly synthesized p50 and p52 NF-κB subunits in macrophages challenged with bacterial lipopolysaccharide. Chapter 3 describes the molecular architecture of p105 and p100 complexes. Experimentally determined composition and biochemical analysis of protein-protein interactions led to the proposal of stoichiometric model for p105 and p100 complexes that accounts for high MW and heterogeneity of these molecular

assemblies. Chapter 4 is focused on p105 and p100 proteolysis. p105 and p100 undergo regulated proteolysis that generates p50 and p52 NF-κB subunits, respectively. The mechanism of p105 and p100 processing is discussed in the last chapter of this thesis.

Chapter 1

Introduction

The term “signal transduction” in biological applications refers to any process by which a cell converts one kind of signal or stimulus into another. Mammalian species use over 3000 signaling proteins to build hundreds of cell-specific signaling systems. Many of the signaling components have multiple upstream regulators and downstream targets, creating a web of connectivity within and between signaling pathways (Brandman and Meyer, 2008). Transcription factors are the important components of intracellular signal transduction systems (Lalli and Sassone-Corsi, 1994). Gene expression due to activation of transcription factors leads to multitude of cellular effects. One group of activated genes encodes secreted proteins that function as additional stimuli on the signal transduction pathway. Cytokines, the mediators of inflammation, are the examples of proteins in the first group. The second group includes the products of genes encoding transcription factors themselves. Transcription factors produced as a result of a signal transduction cascade can, in turn, activate yet more genes orchestrating complex physiological events. And the third group of activated genes includes the regulatory molecules that act upon the components of the signal transduction pathway and provide the temporal regulation for the strength of the signaling. The latter gene products often downregulates the signaling and thus constitute the negative feedback loops in the signaling pathway. The presence of multiple feedback loops in signaling systems (Freeman, 2000) poses a challenge to understanding how diverse signals control cellular behavior.

Biochemical approach is used to study the chemical properties of important biological molecules involved in signal transduction. In particular, biochemistry provides the tools to assess the dynamics of binding interactions between components of signal transduction pathways. Although the biochemical techniques remain laborious and costly, the experiments utilizing the

biochemical approach, could yield highly annotated data on the signaling components and their functions. The systems biology approach is also applied to problems related to signal transduction. The latter approach involves the development of mechanistic models reconstructing the dynamic systems from the quantitative properties of their elementary building blocks. These models require the large number of parameters, variables and constraints of the cellular networks and are handled computationally (Karlebach and Shamir, 2008). In many cases, however, the regulatory relationships between network components of the identities of the components themselves have not been established, and therefore need to be derived experimentally.

The transcription factor nuclear factor kappaB (NF-κB) participates in signal transduction. Owing to the diversity of regulatory mechanisms acting on the NF-κB signaling module the signal transduction via NF-κB remains a challenging area of research both experimental and theoretical. NF-κB denotes a group of structurally related dimeric transcription factors that share the ability to specifically bind DNA and regulate gene expression. Transcriptional activity of NF-κB is regulated by a group of proteins called IκB (inhibitors of NF-κB). When cells are treated with NF-κB stimuli, like bacterial lipopolysaccharide (LPS), the "upstream" components of NF-κB signaling system act upon IκB proteins and induce their degradation. The mammalian NF-κB signaling system (at the level of NF-κB and IκB proteins) consists of five NF-κB subunits: RelA, c-Rel, RelB, p50, and p52, and five proteins with IκB activity: IκBα, IκBβ, IκBε, p105, and p100 (Fig. 1.1). NF-κB proteins are characterized by the presence of the Rel homology domain (RHD). RHD is responsible for dimerization and DNA binding of NF-κB. IκB proteins, on other hand all share the conserved ankyrin repeat domain (ANK). The characteristic functional property of ANK domain is its ability to bind NF-κB dimers (or RHD dimers). NF-κB and IκB families of proteins are evolutionarily conserved signaling molecules (Table 1.1). The proteins orthologous to mammalian NF-κB and IκB are found in

distant invertebrate species and were shown to regulate the development and the innate immune response in these organisms (Fan et al., 2008; Ferrandon et al., 2004).

Notably, p50 NF-κB subunit is produced from the N-terminal half of p105. Similarly, p52 NF-κB subunit the N-terminal processed product of p100 precursor protein (Fig.1.1). The proteolytic events that generate p50 and p52 NF-κB subunits are catalyzed by proteasome and are accompanied by the complete degradation of C-terminal halves of p105 and p100. Interestingly, the C-terminal halves of p105 and p100 have homology to classical IκB proteins, IκBα, IκBβ, IκBε. Because of this homology and based on the ability of p105 and p100 to interact with NF-κB, p105 and p100 are also classified as IκB proteins (Fig. 1.1).

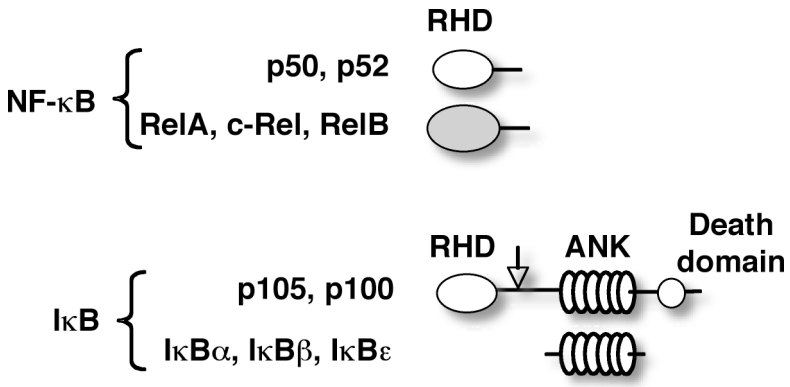

Figure 1.1 Domain organization of NF-κB and IκB proteins

NF-κB family of proteins includes p50, p52, RelA, c-Rel, and RelB (top panel). NF-κB proteins are characterized by the presence of RHD domain. IκBα, IκBβ, IκBε, p105, and p100 belong to IκB family of proteins (bottom panel), ANK domain is characteristic feature of IκB proteins. p105 and p100 also contain C-terminal Death domain and N-terminal RHD domain. Separate from their function as IκB, p105 and p100 IκB proteins also serve as the precursors for p50 and p52 NF-κB subunits.

RHD, Rel homology domain; ANK, ankyrin repeat domain. Arrow indicates site of proteolysis in p105 and p100 proteins that yields p50 and p52, respectively.

Table 1.1 NF-κB and IκB proteins from evolutionarily distant organisms

Organism	Group	Conserved Domains	Protein	protein REFSEQ
Human	NF-kB	RHD	RelA	NP_068810.2
[H. sapiens]			c-Rel	NP_002899.1
			RelB	NP_006500.2
	classical IkB	ANK	IkBa	NP_065390.1
			IkBb	NP_002494.2
			IkBe	NP_004547.2
	NF-kB precursors	RHD, ANK, Death	p105	NP_003989.2
			p100	NP_001070962.1
Sea squirt	NF-kB	RHD	rel1	NP_001029013
[C. intestinalis]	classical IkB	ANK	IkappaB	NP_001071739
	NF-kB precursors	RHD, ANK, Death	NFkB	NP_001071772.1
Sea urchin	NF-kB	RHD	similar to c-Rel	XP_780741
[S. purpuratus]	classical IkB	ANK	similar to IkB	XP_780345
	NF-kB precursors	RHD, ANK, Death	NFkB	NP_999819.1
Fruit fly	NF-kB	RHD	Dorsal	NP_724052.1
[D. melanogaster]			DIF	NP_523589.2
	classical IkB	ANK	Cactus	NP_723960.1
	NF-kB precursors	RHD, ANK	Relish	NP_477094.1

Three NF-κB activation pathways have been discriminated. These pathways differ in respect to the activating kinases and specific IκB molecules involved (Scheidereit, 2006) (Fig. 1.2). The canonical NF-κB pathway is activated by inflammatory cytokines, pathogen-associated molecules, including LPS, and other stimuli, and involves phosphorylation of classical IκB (IκBα, IκBβ, and IκBε) by an inhibitor of NF-κB kinase complex (IKK). IKK complex consists of two protein kinases, IKK1 and IKK2, and a regulatory particle, NF-κB essential modulator (NEMO). The activity of IKK2 is required for activation of canonical pathway. Phosphorylation of IκB by IKK2 leads to degradation of IκB and the release of NF-κB dimers from the inhibition. NF-κB dimers bind DNA at specific sites and activate gene expression (Fig. 1.2, left panel). It is thought that a distinct class of physiological stimuli (including LTβ, see chapter 4 for this example) triggers the non-canonical NF-κB pathway. The activation of the non-canonical NF-κB

pathway, as oppose to the canonical pathway, requires the kinase activity of IKK1. IKK1 phosphorylate p100 at C-terminal serine residues leading to proteasomal degradation of the C-terminal portion of p100 and the generation of p52 NF-κB subunit corresponding to the N-terminal half of p100 molecule. The p52:RelB heterodimer is thought to be the nuclear effectors of the non-canonical pathway (Fig. 1.2, middle panel). The third pathway, also known as the p105 pathway, is called "atypical". The atypical pathway, conceptually, is very similar to the canonical NF-κB pathway. It is triggered by the same stimuli (LPS, for example), mediated by IKK1, and requires complete proteasomal degradation of p105 in a manner similar to classical IκB (Fig. 1.2 right panel) (Sun and Ley, 2008).

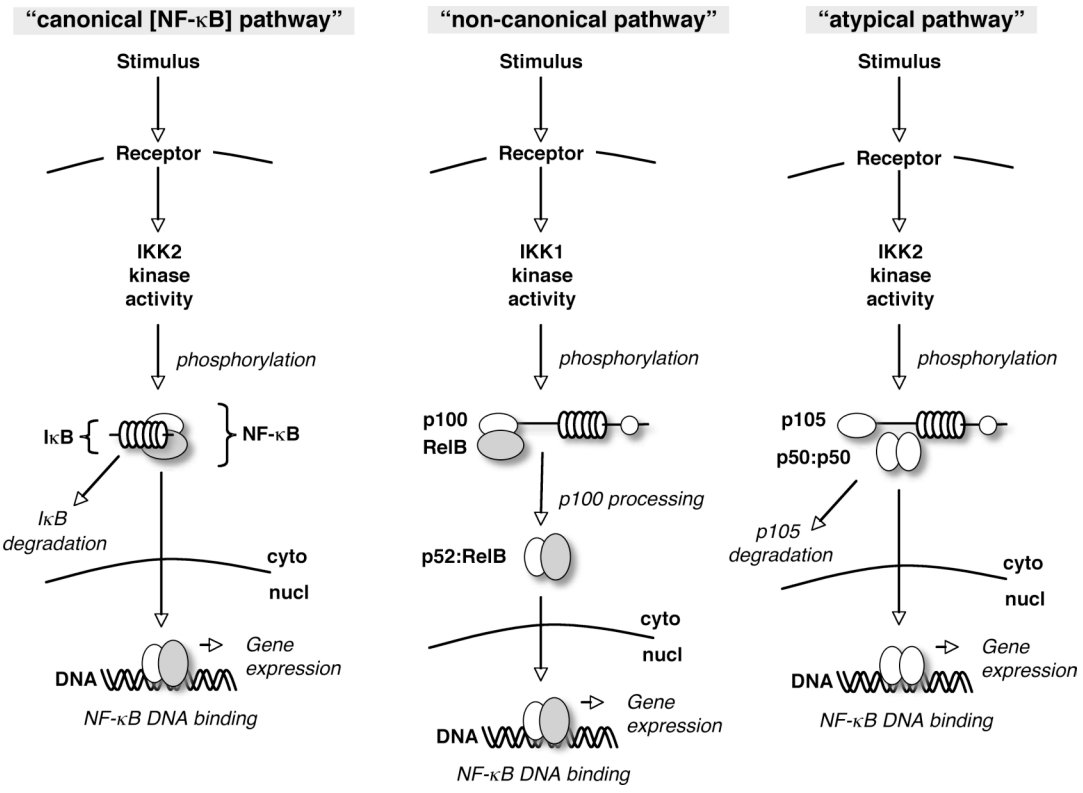

Figure 1.2 Regulation of NF-κB transcriptional activity

IκB proteins regulate NF-κB activity. Three distinct NF-κB pathways: "canonical" (left panel), "non-canonical" (middle panel), and "atypical" (right panel) are schematically shown.

As shown in Fig 1.2, p105 and p100 function as the inhibitors of the "atypical" and non-canonical NF-κB pathways, respectively (Mercurio et al., 1992; Rice et al., 1992). Moreover, activation of NF-κB also regulates the transcription of genes encoding p105 and p100. Thus, p105 and p100 proteins are positioned as the important components in NF-κB signaling system. They are the precursors, the inhibitors, and, are, likely, the negative feedback regulators of NF-κB.

The function of p105 and p100 in NF-κB signaling pathway remains an interesting area of research. In particular, the mechanisms of p105 and p100 processing to generate p50 and p52 NF-κB subunits were investigated in great detail (for review see (Beinke and Ley, 2004)). We aimed to advance an understanding of p105 and p100 as inhibitors of NF-κB signaling by providing a detailed biochemical description of p105 and p100 complexes with other NF-κB subunits, and their dynamics during LPS signaling in macrophages.

We suspected that because p105 and p100 proteins combine the structural domains of both NF-κBs and IκBs, the mechanism of NF-κB inhibition by p105 and p100 may be more complicated than previously anticipated from the similarity of the C-terminal ANK domains of p105 and p100 to classical IκB like IkBα (Mercurio et al., 1992; Rice et al., 1992). Here we report that, apparently, 100% of cytoplasmic p105 and p100 form oligomeric ~600kD complexes that incorporate other NF-κB subunits. p105 and p100 complexes appear to regulate at least half of the p50 and p52 pools in macrophages, and can be described as providing a "buffering" binding capacity for the *de novo* synthesized NF-κB post-LPS stimulation. Based on biochemical evidence, we constructed the stoichiometric model for p105 and p100 complexes, which accounts for their high molecular weight (MW) and compositional heterogeneity. We introduced the term NF-κBsomes to refer to the large, oligomeric, endogenous p105 and p100 complexes. We suggest that the introduction of a novel entity in the NF-κB signaling module, a NF-κBsome, which

functions to inhibit the second phase of NF-κB signaling, will help to understand the auto-regulatory properties of this signaling system.

Chapter 2

Endogenous p105 and p100 complexes

2.1. Introduction

In the set of experiments described in this chapter we aimed to characterize p105 and p100 as the cytoplasmic inhibitors of NF-κB. We used cytoplasmic extracts of macrophage cells as a source of endogenous proteins. Bacterial lipopolysaccharide (LPS) was used to activate NF-κB pathway in macrophages. Macrophages detect LPS because of the cell surface expression of Toll-like receptor 4 (TLR4). TLR4 in macrophages transduces activation signals to all three NF-κB pathways. In addition, TLR4 activate several other signal transduction pathways (Kawai and Akira, 2007). Thus, we used cultured macrophages as a model system to study the composition of the p105 and p100 complexes.

NF-κB plays important role in the innate immune response of macrophages against invading bacteria. Signaling through TLR4, the receptor for LPS, was also shown to be negatively involved in the pathogenesis of atherosclerosis (Michelsen et al., 2004), the latter study suggesting that the innate immune response facilitated by the activated macrophages could be detrimental for human health. Therefore, while the rapid activation of NF-κB via proteasomal degradation of inhibitor proteins is essential for NF-κB signaling in macrophages fighting bacterial pathogens, the ability to switch off the expression of potentially damaging pro-inflammatory and/or proliferative genes is also important to protect from undesired inflammation (Karin and Lin, 2002; Yan and Hansson, 2007).

The down-regulation of the activity of signal transduction pathways, like NF-κB, often is facilitated by the negative feed-back signaling (Brandman and Meyer, 2008). One of the well-characterized mechanisms of the down-regulation of NF-κB activity post-stimulation entails the

expression of *ikba* gene encoding the classical IκB protein, IκBα (Scott et al., 1993). Expression of p100 protein (encoded by the *nfkb2* gene) also has been shown to down-regulate NF-κB activity in T cells, possibly controlling the duration of T cell receptor signaling (Legarda-Addison and Ting, 2007). The role of p105 (encoded by the *nfkb1* gene) as a negative regulator of NF-κB signaling, however, has not as yet been defined, although it is know that the expression of *nfkb1* gene is activated in an NF-κB-dependent manner (Ten et al., 1992).

We characterized the endogenous p105 and p100 complexes from macrophages and found that both proteins form high molecular weight (MW) complexes with all other NF-κB subunits. Next we addressed the question whether p105 and p100 NF-κB inhibitors participate in the negative feedback regulation of NF-κB signaling. We analyzed and compared the high MW cytoplasmic NF-κB complexes at different times after LPS stimulation. We found that at least 50% of p50 and p52 NF-κB subunits partitions into high MW complexes after LPS stimulation of macrophages. Thus, our experiments led to the conclusion that p105 and p100 function as the potent negative regulators of NF-κB signaling in macrophages post LPS stimulation.

2.2. Material and methods

Cell Culture

RAW264.7 (Raschke et al., 1978), THP-1 (Tsuchiya et al., 1980) cell lines and mouse bone marrows (ALS strain) were provided by A. Savinov (BIMR, La Jolla, CA). BMDM were derived by L929 protocol (adapted for mouse tissues) as previously described (Boltz-Nitulescu et al., 1987). L929 cells were from ATCC. Wild type; *ikba-/-,ikbb-/-,ikbe-/-*; and *nfkb1-/-,nfkb2-/-* mouse embryonic fibroblasts (MEF) were a gift from A. Hoffmann (UCSD, La Jolla, CA). All cell cultures, except THP-1, were pre-incubated with media containing 0.5% serum (low serum) for 36 hours before LPS stimulation; low-serum media was used for LPS treatment and chase periods. THP-1 monocytes were differentiated into macrophage-like cells with 50ng/ml (31nM) PMA for 48 hours (Tsuchiya et al., 1982), rested 48 hours with daily replenishment of media and stimulated with LPS in media containing 10% serum.

Cytoplasmic and Nuclear Fractionation

Cytoplasmic sample were prepared from 90% confluent adherent cell cultures. Cells were lysed in at least 2 cell pellet volumes of CE buffer: 10mM HEPES-KOH, pH7.9; 60mM KCl; 1mM EDTA; 0.5% NP-40; 1mM DTT, supplemented with Protease Inhibitor Cocktail. After collecting cytoplasmic fraction (by centrifugation at 500xg) nuclei were washed with five pellet volumes of CE and lysed in three pellet volumes of NE buffer: 250mM Tris-HCl, pH7.5; 60mM KCl; 1mM EDTA; and 1mM DTT supplemented with Protease Inhibitor Cocktail.

Gel Filtration Chromatography of Cytoplasmic Extracts

Cytoplasmic samples for analytical gel filtration were prepared from 350cm2 of 90% confluent adherent cell cultures (equivalent to two ∅150mm plates). 200µl of each sample,

0.2μm filtered and normalized for protein concentration, were resolved on a Superose 6 analytical column in 140mM NaCl; 25mM Tris-HCl, pH7.5; 1mM DTT at 0.5ml/min flow rate using AKTA purifier 10 (GE Healthcare). 250 or 500μl fractions were collected and 15-30μl from each fraction shown was analyzed by Coomassie staining and western blotting. For preparative gel filtration we scaled up sample preparation and injected 3ml of cytoplasmic extract (24 mg of total protein) into a HiLoad 16/60 prep grade column packed with Superdex 200 gel filtration resin. The column was developed with 140mM NaCl, 25mM Tris-HCl, pH7.5, 1mM DTT, 1mM EDTA, 1mM PMSF at a flow rate of 1ml/min using AKTA purifier. 2.5 ml fractions were collected and 210μl from each fraction shown was used to precipitate NF-κB and IκB proteins.

Antibody and other Reagents

Antibodies against RelA (sc372; sc372G), c-Rel (sc71; sc71G), RelB (sc226), p105/p50 (sc7178), IκBα (sc371), IκBβ (sc946), and IκBε (sc7176) were from Santa Cruz Biotechnology; p100/p52 (05-361) was from Upstate Cell Signaling Solutions. p105/p50 (#1157), p100/p52 (#1495), and p105-C (#1140) rabbit antisera were a kind gift from N. Rice (NIH, Bethesda, MD). Protease Inhibitor Cocktail (P8849), LPS (L6529) was from Sigma. Gel filtration standards (151-1901) were from BioRad Laboratories. Gel Filtration column Superose 6 10/300 GL (17-5172-01) was from Pharmacia. All other reagents were from commercial suppliers.

Western Blotting and Immunoprecipitations

For detection of human p105/p50 and p100/52 by western blotting we used commercial rabbit polyclonal p105/p50 (sc7178) and mouse monoclonal p100/p52 (05-361) antibodies. Murine p105/p50 and p100/52 were detected using p105/p50 (#1157) and p100/p52 (#1495) rabbit antisera. Other NF-κB subunits and IκB proteins were detected by a panel of commercially available rabbit polyclonal antibodies as listed in Antibody and other Reagents section. To

immunoprecipitate p105 from gel filtration fractions we used p105-C (#1140) rabbit polyclonal antisera raised against C-terminal peptide of human p105 (0.1μl per reaction). To precipitate RelA and c-Rel, goat polyclonal antibodies RelA (sc372G) and c-Rel (sc71G) were used at 0.2μg per reaction. RelB and IκBa were immunoprecipitated with 0.2mg of rabbit polyclonal anti-RelB (sc226) and anti-IκBα (sc371) antibodies per reaction. Each immunoprecipitation reaction was supplemented with 50mg/ml of bovine serum albumin to normalize for total protein content and performed according to standard immunoprecipitation protocol (Perr, 2008).

2.3. Results

2.3.1. Molecular weight distribution of endogenous NF-κB and IκB proteins

p105 and p100 functionally belong to the IκB family of proteins, but they share sequence similarity with both classical IκBs (IκBα, IκBβ, and IκBε) and NF-κBs (RelA, c-Rel and RelB) because of the presence of an RHD and ANK domains (Fig. 1.1). Thus, it is reasonable to suggest that p105 and p100 interact with other NF-κB subunits in both an "NF-κB"-like and "IκB"-like manner, utilizing their RHD and ANK domains, respectively (Fig. 2.1). To investigate these complex protein interactions we fractionated cytoplasmic extracts of RAW264.7 macrophages by gel filtration chromatography and established the gel filtration profiles for all NF-κB subunits and IκB proteins using a panel of antibodies. We observed that p105 and p100 are detected in high MW fractions (600-700kDa) distinct from lower MW fractions containing IκBα, IκBβ, and IκBε. NF-κB subunits RelA, c-Rel and p50 were distributed over a wide range of gel filtration fractions, overlapping with p105 and p100 in high MW fractions, and with IκBα, IκBβ, and IκBε in the lower MW fractions. On the other hand, RelB and p52 preferentially partitioned to high MW fractions, which also contained p105 and p100 (Fig. 2.2).

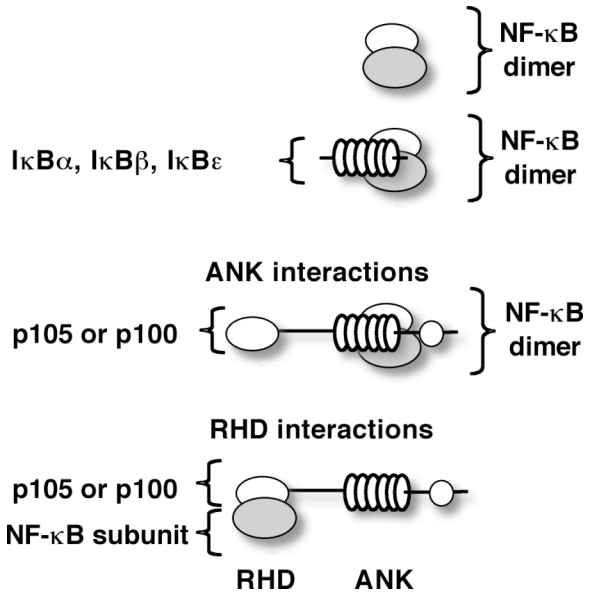

Figure 2.1 RHD and ANK domain interactions

RHD and ANK domain interactions of NF-κB and IκB proteins are schematically shown.

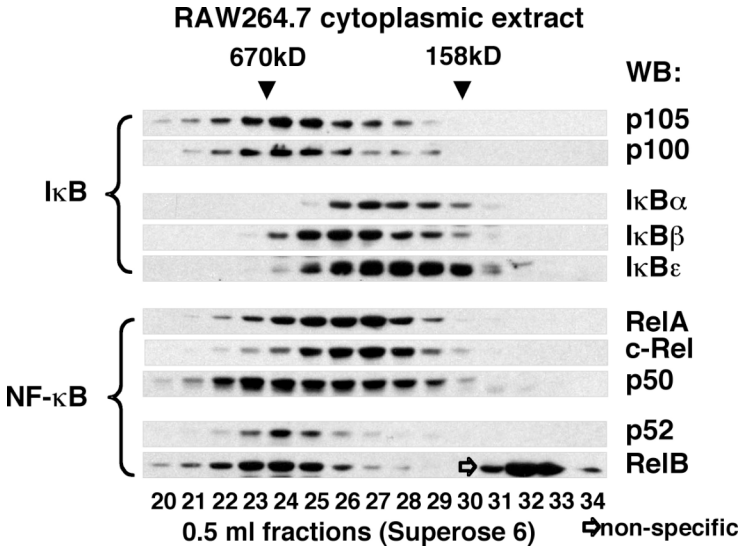

Figure 2.2 Fractionation of endogenous IκB and NF-κB complexes by gel filtration chromatography

Cytoplasmic extract of RAW264.7 cells was analyzed by gel filtration chromatography on a Superose 6 column. IκB and NF-κB proteins were detected in the resulted fractions by western blotting (WB) with the panel of IκB and NF-κB-specific antibodies.

2.3.2. Physical interaction between NF-κB and IκB proteins in higher and lower molecular weight complexes

To evaluate the physical interaction of NF-κB subunits with IκB proteins and with each other, we fractionated RAW264.7 cytoplasmic extract on a preparative gel filtration column and immunoprecipitated p105, IκBα, RelA, c-Rel, and RelB from the resulting fractions. Immunoprecipitated proteins and their binding partners were detected by western blotting using a panel of antibodies (see flowchart, Fig. 2.3). Immunoprecipitation of p105 and IκBα from gel filtration fractions showed that p105 specifically interacts with RelA and c-Rel in high MW gel filtration fractions, while IκBα interacts with RelA and c-Rel in lower MW fractions (Fig. 2.4). Direct immunoprecipitation of RelA and c-Rel, however, resulted in the detection of RelA and c-Rel in both the high and the low MW fractions. We concluded from these observations that cytoplasmic RelA and c-Rel are indeed distributed between the larger, p105-containing complexes, and the smaller complexes containing classical IκBs.

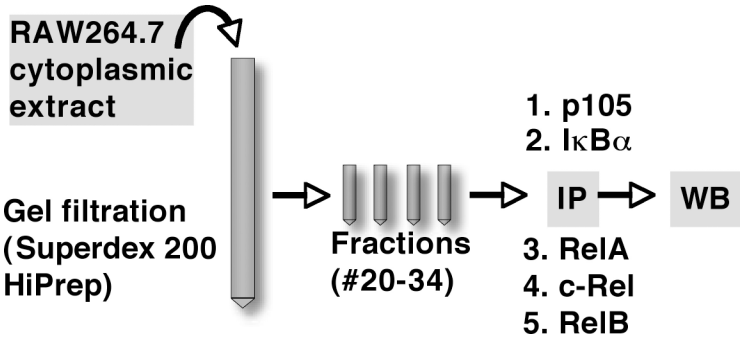

Figure 2.3 Detection of physical interactions of IκB and NF-κB proteins by gel filtration chromatography followed by immunoprecipitation (Flowchart of the experiments)

Cytoplasmic extract of RAW264.7 cells was first fractionated by gel filtration chromatography. IκB and NF-κB proteins were then immunoprecipitated (IP) from the resulting fractions using antibodies specific for p105, IκBα, RelA, c-Rel, or RelB. Protein complexes immunoprecipitated from each fraction were analyzed by western blotting with a panel of NF-κB and IκB-specific antibodies (WB). Flowchart illustrates experiments shown in Fig. 2.4 and Fig. 2.7.

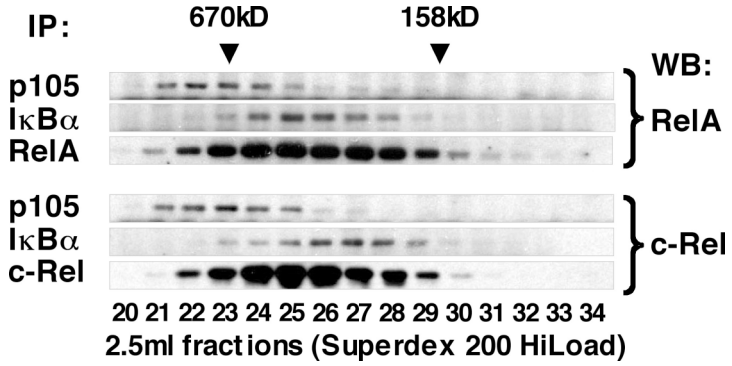

Figure 2.4 Detection of endogenous high MW p105 complexes with RelA and c-Rel

Cytoplasmic extract of RAW264.7 cells was fractionated by gel filtration. p105 and IκBα were immunoprecipitated (IP). RelA (top panels) and c-Rel (bottom panels) were detected in p105 and IκBα immunoprecipitates by western blotting (WB).

Specificity of the RelA and c-Rel co-precipitation with p105 and IκBα was controlled by the direct RelA (top panels, WB: RelA) and c-Rel (bottom panels, WB: c-Rel) IP.

2.3.3. Genetic evidence in support of functional significance of high molecular weight NF-κB complexes

Based on the ability of p105 and p100 to compensate for the cytoplasmic retention of NF-κB in the absence of classical IκB proteins (Tergaonkar et al., 2005), we predicted that in the genetic model that recapitulates the absence of the classical IκB proteins (Basak et al., 2007) more RelA, c-Rel, and p50 will be associated with the high MW complexes compared to the wild type (wt) cells. To test this prediction we fractionated the cytoplasmic extracts of *ikba-/-, ikbb-/-, ikbe-/-* triple knockout mouse embryonic fibroblasts (MEF) and observed a shift in RelA, c-Rel, and p50 retention volumes towards higher MW fractions, compared to the wild type cells (Fig. 2.5A). In a separate experiment we confirmed that p50 and p52 NF-κB subunits co-fractionated with p105 and p100 in triple knockout MEF (*ikba-/-, ikbb-/-, ikbe-/-*) and were detected in high

MW gel filtration fractions suggesting that they partition into high MW complexes and interact with p105 and p100 (Fig. 2.6A). The physical interaction of RelA with the high MW p105 and/or p100 in *ikba-/-,ikbb-/-,ikbe-/-* MEF was also detected by co-immunoprecipitation (Fig. 2.6B).

The results from *ikba-/-,ikbb-/-,ikbe-/-* triple knockout MEF showed that the large p105 and/or p100 complexes, detected by gel filtration, are not an artifact of fractionation experiments, but represent the physiologically relevant molecular assemblies, specifically because these complexes were found to be responsive to genetic alterations in a predictable manner.

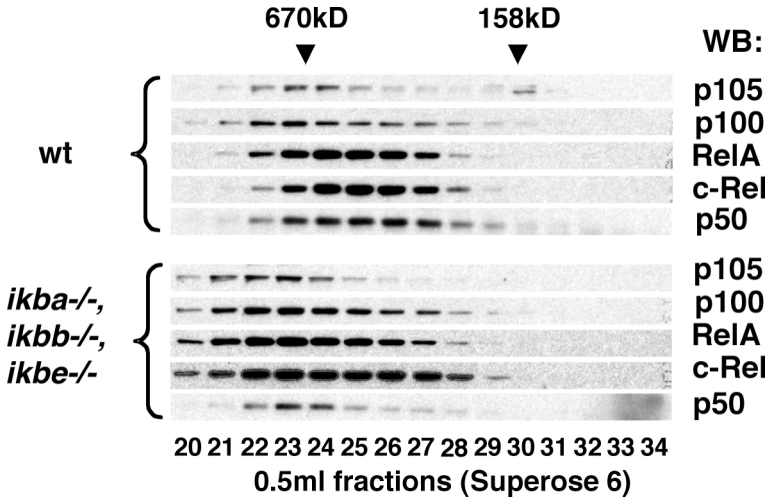

Figure 2.5 Endogenous NF-κB subunits partition into high MW complexes in the absence of classical IκBs

MW distribution of endogenous p105, p100, RelA, c-Rel, and p50 subunits was analyzed by western blotting (WB) after gel filtration chromatography of cytoplasmic extracts from wild type (wt) and *ikba-/,ikbb-/-,ikbe-/-* MEF.

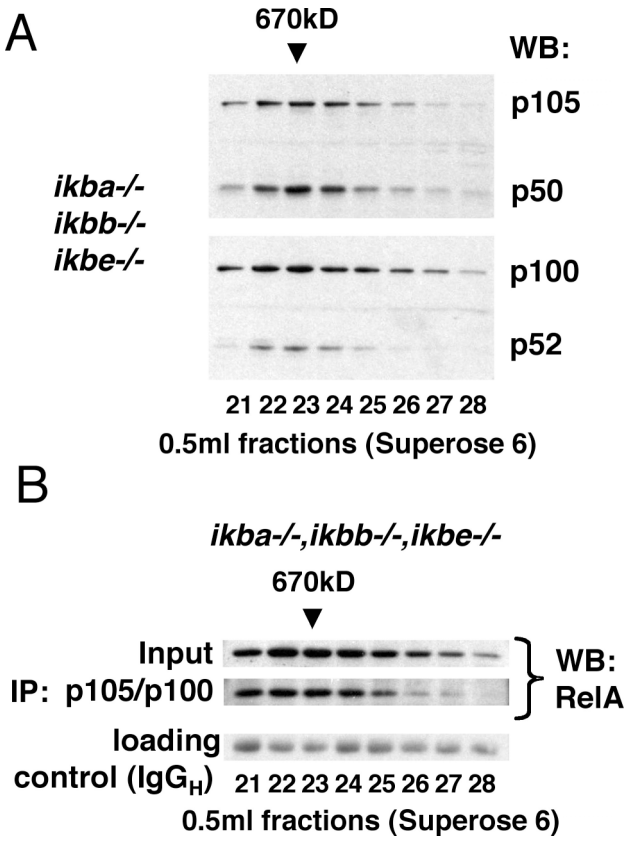

Figure 2.6 Endogenous NF-κB subunits interact with p105 and p100 in the absence of classical IκBs

(A) Cytoplasmic extract of *ikba-/,ikbb-/-,ikbe-/-* MEF was fractionated by gel filtration. p105, p50 (top panel), p100, and p52 (bottom panel) were detected in high MW gel filtration fractions by western blotting (WB).

(B) RelA was immunoprecipitated (IP) from high MW gel filtration fractions of cytoplasmic extract of *ikba-/,ikbb-/-,ikbe-/-* cells (as in panel A) using a mixture of antibodies specific for p105 and p100.

2.3.4. Compositional heterogeneity of high molecular weight p105 and p100 complexes

Immunoprecipitation of RelB (the NF-κB subunit that exclusively partitions to high MW fractions, Fig. 2.2) resulted in co-precipitation of RelA and c-Rel. p105 and p100 were also detected in RelB immunoprecipitates (Fig. 2.7, upper panel). The reciprocal immunoprecipitation

of RelA and c-Rel showed that complexes containing these two NF-κB subunits were also present in lower MW fractions (Fig. 2.7, lower panels), confirming that the co-immunoprecipitation of RelA and c-Rel with RelB from high MW fractions was specific. Co-immunoprecipitation of RelA, c-Rel, p105 and p100 with RelB was interesting because it suggested that RelA and c-Rel interact with RelB as components of high MW p105 and/or p100 complexes. This idea is also supported by our observation of the specific interactions of p105 with RelA and c-Rel in high MW fractions (Fig. 2.4), and by the sequential immunoprecipitation experiments of Mercurio and colleagues (Mercurio et al., 1993), the results of which also suggested that p105, p100 and RelA engage in higher order complexes, different from a simple heterodimer.

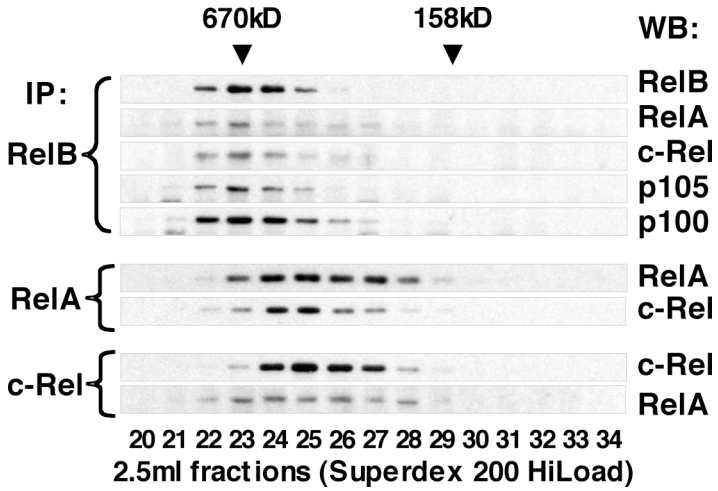

Figure 2.7 Compositional heterogeneity of high MW p105 and p100 complexes

Cytoplasmic extract of RAW264.7 cells was fractionated by gel filtration. RelB was immunoprecipitated (IP) from gel filtration fractions. RelA, c-Rel, p105, and p100, co-precipitated with RelB, were detected by western blotting (top panels, IP: RelB) (WB).

Specificity of the RelA and c-Rel co-precipitation with RelB was controlled by the direct reciprocal RelA and c-Rel IP (bottom panels, IP: RelA and c-Rel).

2.3.5. Dual role for p105 complexes in LPS signaling in macrophages

We next tested if the high MW p105 complexes participate in NF-κB signaling. We treated THP-1 cells (differentiated by PMA protocol) with 0.2μg/ml LPS for 40 minutes and analyzed the amount and MW distribution of cytoplasmic p105, p50 and IκBα by gel filtration chromatography and western blotting at different time points after stimulation. We determined that the previously described (Salmeron et al., 2001) inducible degradation of p105 (Fig. 2.8A) does indeed target high MW p105 complexes (Fig. 2.8B). The reduction in p105 levels two hours after LPS stimulation correlated with the decrease of p50 in high MW fractions (Fig. 2.8B), suggesting that the degradation of p105 releases p50 from high MW complexes and, thus, contributes to LPS-induced NF-κB signaling in the nucleus (Fig. 2.8A). Six hours after LPS treatment, however, the amounts of p105 and p50 in high MW fractions were partially restored; and no additional accumulation of p50 in the nucleus was detected (compared to two hours), implying that newly synthesized p105 assembles with p50 into inhibited cytoplasmic complexes (Fig. 2.8A&B). Similarly, we observed accumulation of p50 subunits in high MW cytoplasmic complexes six hours after LPS stimulation of bone marrow-derived macrophages (BMDM) (Fig. 2.9).

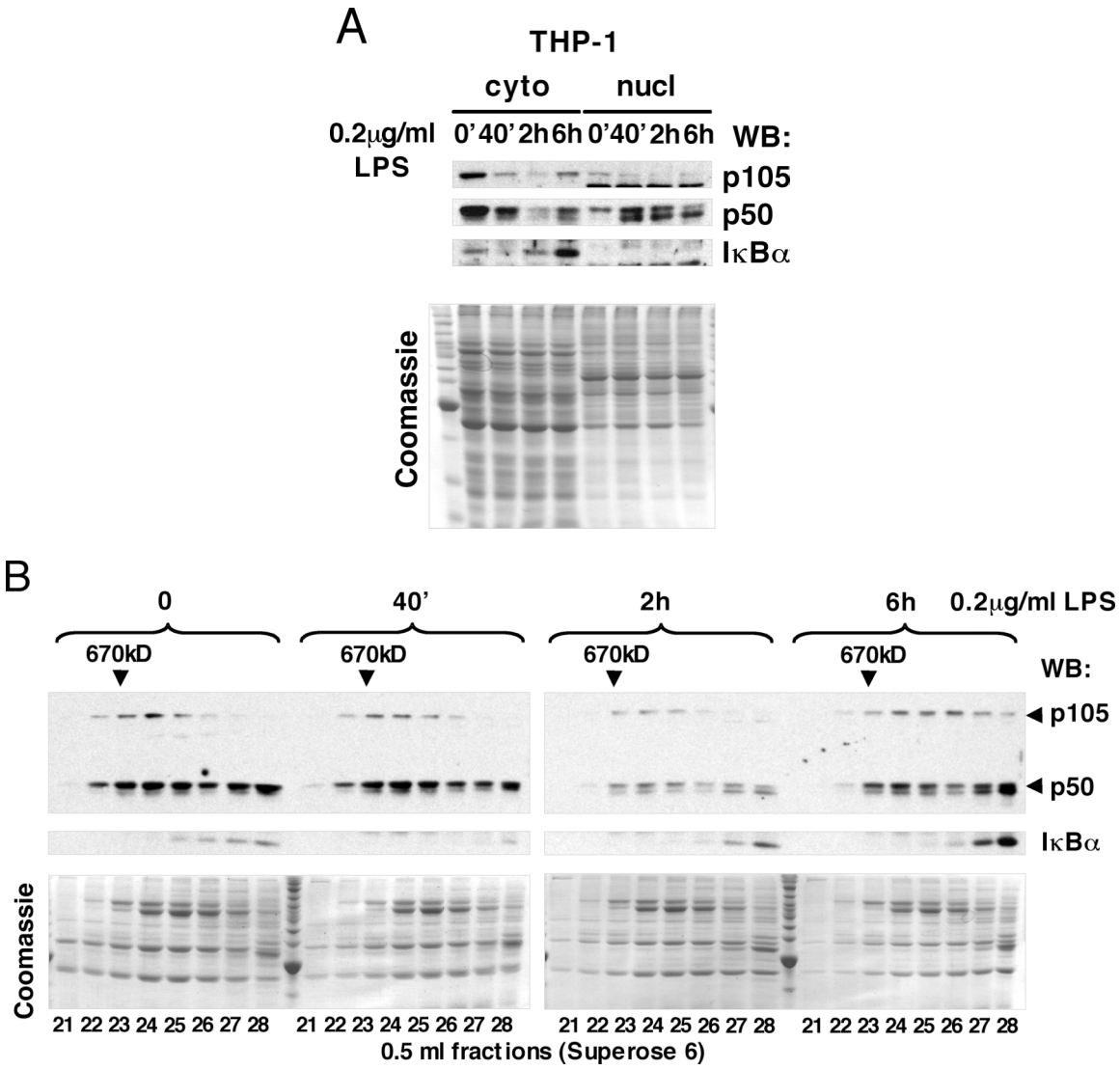

Figure 2.8 High MW endogenous p105 complexes are stimulus-responsive

(A) THP-1 cells were stimulated with 0.2μg/ml LPS for 40min. Cytoplasmic (cyto) and nuclear (nucl) extracts were prepared at indicated time points and analyzed by western blotting (WB) to detect p105, p50, and IκBα.

(B) Cytoplasmic extracts of THP-1 cells (as in A) were further fractionated by gel filtration chromatography and analyzed by WB to detect p105, p50, and IκBα.

*Coomassie staining (in parallel with WB) provided controls for equivalent loading and for the efficiency of fractionation.

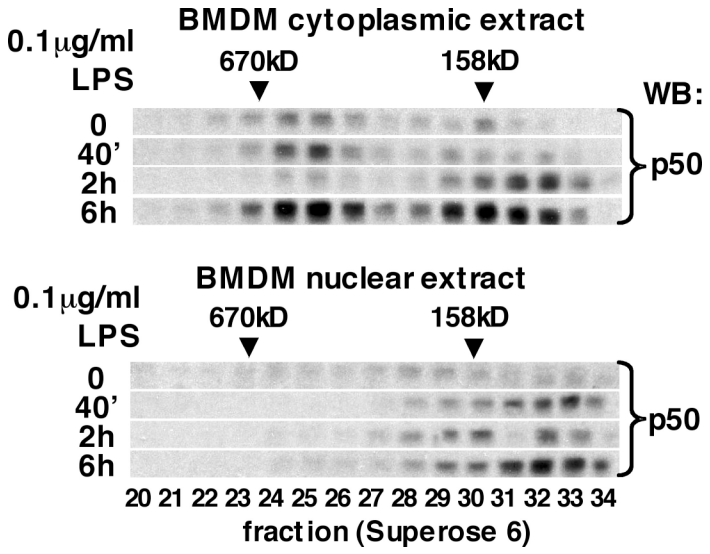

Figure 2.9 Endogenous p50 accumulate in high MW complexes post-LPS stimulation

MW distribution of endogenous p50 was analyzed by gel filtration chromatography of cytoplasmic (top panels) and nuclear (bottom panels) extracts from bone marrow derived macrophages (BMDM) treated with 0.1μg/ml LPS for 40 minutes. p50 was detected by western blotting (WB).

2.3.6. p52 NF-κB subunits are sequestered in high molecular weight complexes post-LPS stimulation of macrophages

We also examined the state of p100 and p52 in THP-1 cells, and showed that LPS treatment led to an accumulation of p52 both in the nucleus and in the cytoplasm, indicating that LPS signaling stimulates p100 processing (Fig. 2.10A). Gel filtration chromatography of cytoplasmic extracts of THP-1 cells treated with 1μg/ml LPS for 40 minutes showed that newly generated p52 partitions into two pools: one of low MW, that might represent the activated p52; and a second pool that co-fractionates with p100 and might represent the inhibited pool of p52 (Fig. 2.10B). Because p52 accumulation in high MW fractions preceded the detectable re-synthesis of p105, we concluded that this pool of p52 was inhibited by p100 (Fig. 2.10A&B). The stimulating effect of LPS on p100 processing was also observed in THP-1 cells treated with the lower dose (0.2μg/ml) of LPS for 40 minutes and followed for 6 hours (Fig. 2.11). In this experiment we also detected p52 accumulation in high MW fractions, coincident with p100, which was consistent with the inhibitory role of p100 in NF-κB signaling (Legarda-Addison and Ting, 2007), (Shih et al., unpublished observations). It is important to note, that the MW of p52 complexes, which co-fractionated with p100 post-LPS stimulation, was not reduced when compared to the MW of p100 complexes before LPS stimulation (Fig. 2.10B & Fig. 2.11). Thus, it is highly unlikely that the high MW p52 complexes are the "remnants" of p100 complexes. We concluded, therefore, that *de novo* synthesized p100 complexes function to incorporate (and inhibit) p52 subunits, thus attenuating the effect of LPS on gene expression.

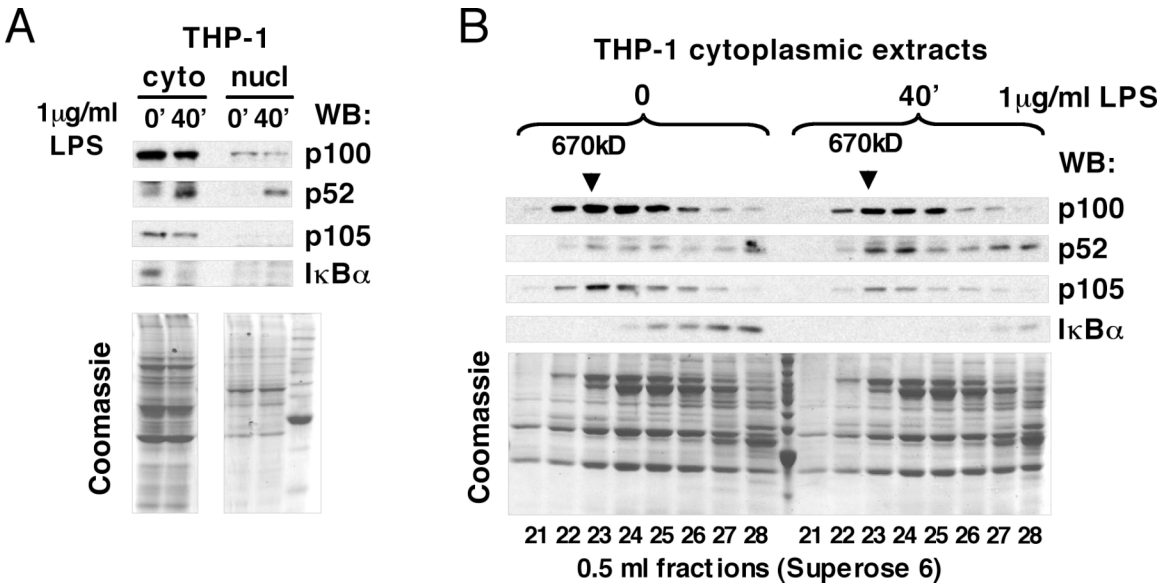

Figure 2.10 Endogenous p52 accumulates in high MW complexes post-LPS stimulation

(A) THP-1 cells were stimulated with 1μg/ml LPS for 40 min. Cytoplasmic and nuclear extracts were prepared before and after stimulation and analyzed by western blotting (WB) to detect p100, p52, p105, and IκBα.

(B) Cytoplasmic extracts of THP-1 cells (shown in A) were fractionated by GF and analyzed by WB to detect p100, p52, p105 and IκBα.

*Coomassie staining (in parallel with WB) provided controls for equivalent loading and for the efficiency of fractionation.

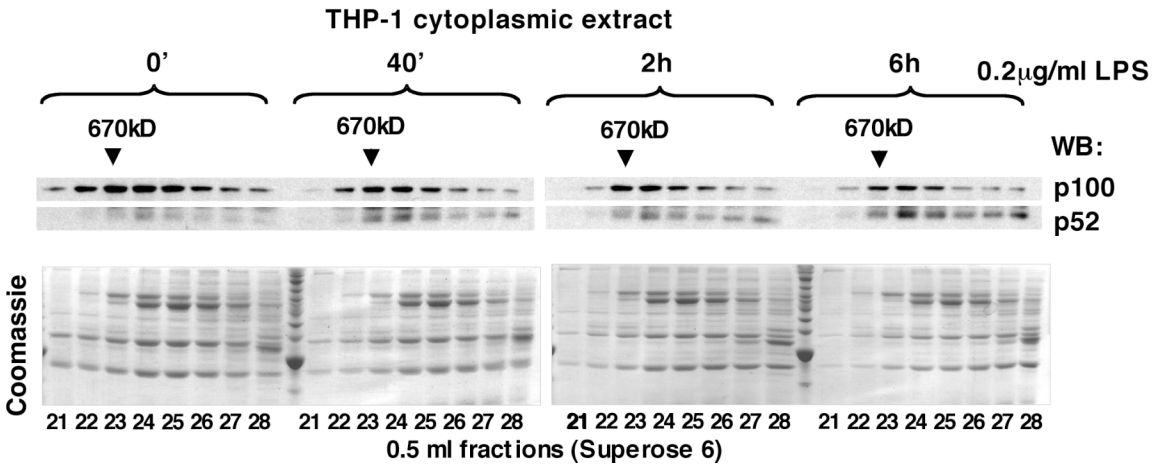

Figure 2.11 Effect of LPS signaling on MW distribution of endogenous p52 in macrophages

THP-1 cells were stimulated with 0.2μg/ml LPS for 40min. Cytoplasmic extracts were prepared at indicated time points and analyzed by gel filtration chromatography followed by western blotting (WB) to detect p100 and p52.

2.4. Discussion

We applied biochemical tools to dissect the contribution of p105 and p100 to binding of the cytoplasmic p50 and p52 NF-κB subunits in macrophages post-LPS stimulation. We concluded that the large MW p105 and p100 complexes retain at least 50% of p50 and p52 NF-κB subunits post LPS-stimulation (Fig. 2.8-2.11). We speculated that p50 and p52 subunits detected in high MW complexes are *de novo* synthesized. In fact, we detected an increase in the amounts of p50 and p52 subunits in high MW complexes at later time points after LPS stimulation of macrophages. Why do we emphasize *de novo* synthesis of NF-κB? Almost two decades ago Hohmann *et al*. showed that the maintenance of NF-κB activity depends on protein synthesis (Hohmann et al., 1991) and discriminated between the early (translation-independent) and the late (protein synthesis-dependent) phases of nuclear NF-κB activity. Their study also showed that the half-life of nuclear NF-κB is about 30 minutes, a observation that is now supported by the finding of multiple NF-κB-specific nuclear ubiquitin ligases, which target nuclear NF-κB to proteasomal degradation (Natoli and Chiocca, 2008). Based on our observations of the dynamics of p50 and p52 accumulation in the high MW complexes we propose that p105 and p100 complexes regulate the second phase of NF-κB signaling, which depends on *de novo* synthesis of NF-κB.

p105 also plays the role of a classical NF-κB inhibitor that degrades in a stimulus-dependent manner, releasing associated NF-κB subunits to function in the nucleus (Fig. 2.8). This classical IκB function of p105 (Salmeron et al., 2001), however, is not easily detectable in all cell lines. We explain this by the delayed kinetics of p105 degradation (compared to IκBα, Fig. 2.8). Thus, the LPS-induced degradation of p105, if measured as a total p105 level, may be masked by p105 synthesis.

Consistent with earlier studies (Mordmuller et al., 2003; Pan et al., 2006; Souvannavong et al., 2007), we detected p100 processing in macrophages in response to LPS stimulation (Fig. 2.10-2.11). The earlier metabolic pulse-chase experiments of Mordmuller et al. (Mordmuller et al., 2003) linked the total p52 accumulation in LPS-treated cells to p100 synthesis. We observed the accumulation of p52 in high MW gel filtration fractions, also containing p100 (Fig. 2.10B & 2.11). Because the MW of these p52 complexes (detected post-LPS stimulation) was not reduced when compared to the MW of p100 complexes (detected before LPS stimulation) it is highly unlikely that these p52 complexes were the "remnants" of pre-existing p100 complexes. We concluded, therefore, that p52 NF-κB subunits detected in the high MW fractions are inhibited by *de novo* synthesized p100 that functions to attenuate the effect of newly generated p52 on gene expression. The resent study by Pan *et al.* supports our conclusion, as they noted strong increase in the p100 protein levels in BMDM within minutes following LPS stimulation (Pan et al., 2006). In a similar manner, p105 or p100 appear to sequester newly synthesized p50 NF-κB subunits post LPS stimulation attenuating the late phase of NF-κB signaling (Fig. 2.12).

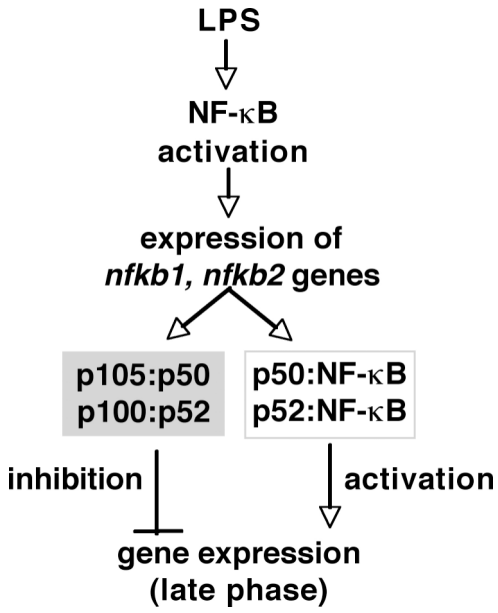

Figure 2.12 Attenuation of late phase of NF-κB signaling in macrophages by p105 and p100

p105 and p100 are *de novo* synthesized in macrophages (activated by LPS), sequester newly generated p50 and p52 NF-κB subunits and attenuate the late phase of NF-κB signaling.

2.5. Chapter 2 acknowledgements

I thank Nancy Rice and Mary Ernst for antibody reagents.

Chapter 2 has been submitted for publication of the material as it may appear in Molecular Cell, 2009. Savinova, Olga V.; Ghosh, Gourisankar. "p105 and p100 NF-κB precursors function as a core of multi-protein heterogeneous NF-κBsomes". The dissertation author was the primary investigator and author of this paper.

Chapter 3

Stoichiometric model for of p105 and p100 complexes

3.1. Introduction

p105 and p100 have dual function in the NF-κB signaling system. In addition to their role as NF-κB precursors, p105 and p100 can function as NF-κB inhibitors (Mercurio et al., 1992; Rice et al., 1992). The multi-domain organization of p105 and p100 reflects their dual function. Because p105 and p100 are the precursors for p50 and p52 NF-κB subunits, their N-terminal RHD domains are identical to the RHD domains of p50 and p52, respectively. On the other hand, the C-terminal ankyrin repeat (ANK) domains of p105 or p100 are homologous to the classical IκB proteins, IκBα, IκBβ, IκBε.

Several research groups have shown that p105 and p100 can indiscriminately interact with all NF-κB subunits (Bouwmeester et al., 2004; Mercurio et al., 1993; Rice et al., 1992). Other studies addressed the specificity of p105 and p100 interactions with NF-κB and suggested that p105 and p100 might serve as specific inhibitors of p50 homodimers and RelB:p52 heterodimers, respectively (Dobrzanski et al., 1995; Liou et al., 1992).

Two mechanistic models of p105 and p100 NF-κB inhibitory complexes have been proposed. It has been suggested, that a stable interaction of RelA or c-Rel with p105 requires their dimerization with RHD of p105, as well as a second contact with the ANK domain of p105. (Rice et al., 1992). This model of binding of p105 to other NF-κB subunits was subsequently generalized and extended to p100 complexes (Mercurio et al., 1993). A more recent study, however, identified and described an alternative mode of binding of p50:RelA dimers to p100 protein (Basak et al., 2007). This latter model suggests that p100 forms homodimers *via* N-terminal RHD; the ANK domain of one p100 molecule "folds back" and interacts with the p100

RHD dimer "platform" in a "self-inhibited" conformation, while the ANK domain of the second p100 molecule extends from the p100 homodimer and inhibits an additional (p50:RelA) NF-κB dimer "in trans" (Basak et al., 2007). The realization that alternative conformations of p100 are possible has contributed to a better understanding of how p100 proteolysis leads to the activation of two NF-κB dimers, RelA:p50 and RelB:p52, that earlier were thought to be activated by the independent NF-κB pathways (canonical and non-canonical) (Basak et al., 2007).

We found that endogenous p105 and p100 assemble into high molecular complexes that incorporate other NF-κB subunits (Chapter 2). The apparent MW of these complexes was greater then would have been predicted by any of the existing models for p105 or p100. We chose to characterize p105 and p100 biochemically to advance the understanding of their regulatory function in NF-κB signaling. We report that p105 could be expressed and purified in an oligomeric form. We speculate that the conserved region in the C-terminal halves of p105 and p100 is responsible for oligomerization of these molecules. The ~600kD recombinant p105 complexes stably incorporate other NF-κB subunits (p50 and RelA) when co-expressed. Based on biochemical evidence, we constructed the stoichiometric model for p105 and p100 complexes, which accounts for their high molecular weight (MW) and compositional heterogeneity.

3.2. Material and methods

Reagents

Antibodies against p105/p50, p100/p52, RelA and IκBα were described in Chapter 2. Anti-FLAG M2 antibody (F3165) was from Sigma. Protease Inhibitor Cocktail (P8849), DOC (D6750), FLAG peptide (F3290), Ni-affinity (P6611), and FLAG-affinity (A2220) resins were from Sigma. GST-affinity resin was from Amersham. TEV protease was purified in house. Gel filtration standards (151-1901) were from BioRad Laboratories. Gel Filtration media, Superdex 200 (17-1047-01), Superdex 75 (17-1044-01) and SP Sepharose FastFlow (17-0729-01); and pre-packed gel filtration column Superose 6 10/300 GL (17-5172-01) were from Pharmacia. All other reagents were from commercial suppliers.

Protein Expression

Mouse p105 cDNA (Ghosh et al., 1990) was used as a template for all p105 cloning except for cloning of p105CTD where human cDNA (IMAGE:6500087) was used. p105 cDNA was cloned into two expression vectors. pEGFP-C1 (Clonetech), in which YFP sequence was replaced by FLAG sequence, was used to express p105 in HEK293T cells. The bacterial expression vector, pHis8, provided by J. Noel (Salk Research Institute, La Jolla, CA) was used to express p105 in *E. coli*. cDNA corresponding to C-terminal fragments of p105, ANK(491-800) and ANK(531-811), was amplified by PCR and cloned into pHis8 and pET15b (Invitrogen) vectors, respectively. pET3a-RelA(19-304) plasmid was previously described (Huxford et al., 1998). Human cDNA corresponding to p100CTD ("C-terminal domain", amino acids 406-899) was cloned into bacterial expression vector pGV67 provided by G. Van Duyne (U. Penn). Human cDNA corresponding to N-terminal p100 fragment, p52 (amino acids 1-341, referred to as "p52" to facilitate discussion), was cloned into pET11a vector (Invitogen). pHis8-p105(1-531) plasmid

was derived from pHis8-p105 by site-directed mutagenesis introducing stop codon. This plasmid was used to express p50 as a product of bacterial proteolysis identical to p50 fragment of p105. Human p105 cDNA corresponding to p105CTD (amino acids 368-969) was cloned into pFastBacHTc baculovirus transfer plasmid (Invitrogen) and introduced into DH10Bac *E. coli* that support recombination of transfer plasmid with bacmid DNA. Bacmid DNA was isolated from DH10Bac and used to transfect HEK293(Phoenix) baculovirus packaging cell line, which produced baculovirus for expression of p105CTD in Sf9 insect cells.

Protein Purifications

FLAG-p105 was purified by FLAG affinity chromatography from HEK293T cells. His-tagged p105, p105 ANK(491-800), p105 ANK(531-811), and p50 were expressed in BL21(DE3) *E. coli* cells and purified by Ni-affinity chromatography followed by gel filtration chromatography. To obtain p105 complex with RelA(19-304), His-tagged p105 was co-expressed with RelA(19-304) in BL21(DE3) *E. coli* cells from plasmids conferring kanamycin and ampicillin resistance, respectively. p105 complex with RelA was purified by Ni-affinity chromatography followed by gel filtration chromatography. Co-expression of p105 with RelA(19-304) in *E. coli* also yielded the lower molecular weight p50:RelA(19-304) complex that was separated from p105:p50:RelA(19-304) complexes at the second step of purification. p52 and GST-p100CTD were expressed in *E. coli* and purified by cation-exchange chromatography and GST affinity chromatography, respectively. p52:GST-p100CTD complex was formed in vitro and, after removal of GST by TEV cleavage, p52:p100CTD complex was re-purified by gel filtration chromatography. p50:(ANK491-800) and p50:(ANK531-811) complexes were formed from purified components in vitro and used directly. p100CTD was re-purified by gel filtration chromatography after removal of GST tag by TEV cleavage. His-tagged p105CTD was purified from Sf9 insect cells by Ni-affinity followed by gel filtration chromatography. Cells expressing

recombinant proteins were disrupted or lysed in buffer suitable for the first step of purification and supplemented with protease inhibitor cocktail. *E. coli* cells were disrupted by sonication. HEK293T cells were lysed in RIPA buffer. Sf9 cells were lysed in 1% TritonX in Ni-affinity buffer. All proteins were purified from soluble fractions of cell lysates. Ni-affinity buffer contained: 140mM NaCl; 25mM Tris-HCl, pH7.5; 10mM Imidazole. Ion-exchange buffer contained: 50 mM NaC;, 25mM Tris-HCl, pH7.5; 1mM DTT. Gel filtration buffer was 140mM NaCl; 25mM Tris-HCl, pH7.5; 1mM DTT. GST-p100CTD purification was performed according to GST affinity resin manufacturer protocol.

Western Blotting

FLAG-tagged p105 was detected by anti-FLAG M2 antibody and by antibody specific for nuclear localization sequence (NLS) peptide of p105 and p50.

Analytical Gel Filtration Chromatography of Recombinant Proteins and Protein Complexes

250-500mg of protein was injected in 200ml volume into 10/300GL columns pre-packed with Superose 6 or Superdex 75 gel filtration resins, except where noted. Columns were developed with 140mM NaCl, 25mM Tris-HCl, pH7.5 at 0.5ml/min. DOC was added to the gel filtration buffer in the indicated experiments. Absorbance at 280nm was monitored. Gel filtration profiles were recorded and analyzed with Unicorn software (Pharmacia). 500µl fractions were collected and 15-30ml from each fraction shown was analyzed by SDS-PAGE.

Dynamic and Static Light Scattering

Dynamic and static light scattering techniques were used to determine the MW of the recombinant p105:p50 complex. Dynamic light scattering (DLS) was performed using a Protein Solutions Dynapro dynamic light scattering instrument over a range of protein concentration of

0.1-1μM (assuming an octomeric model for p105:p50 complex). The absolute MW of the recombinant p105:p50 complex was determined by static light scattering (SLS) using a Wyatt miniDAWN multi-angle light scattering instrument in-line with an analytical gel filtration column and an Optilab rEX RI instrument. MW for the major peak was calculated from light scattering and RI data using ASTRA software (Wyatt Technologies).

Chemical Crosslinking

Purified p105:p50 complexes diluted to 0.25mg/ml were treated with 0.1% glutaraldehyde at room temperature for 15 minuts in standard gel filtration buffer. The extent of crosslinking was determined by 6% PAGE followed by Coomassie staining. The reaction was stopped by the addition of Sodium Borohydride. Crosslinked p105:p50 sample was concentrated to 1.6 mg/ml and homogeneity of the sample was assessed by gel filtration chromatography and by electron microscopy.

Electron Microscopy

p105:p50 sample, chemically crosslinked by glutaraldehyde, was applied to glow-discharged carbon grids at 0.3mg/ml and negatively stained with 2% uranil acetate. Grids were examined in FEI 200KV Sphera microscope. The images were obtained at 80,000x with 0.5-1mm defocus and recorded on 4 megapixel CCD camera (Gatan Ultrascan 1000 UHS). Unprocessed images were used to assess homogeneity of p105:p50 preparation.

Protein Quantitation from Coomassie-stained SDS-PAGE Gels

Analytical amounts of protein were resolved by denaturing 10% PAGE and stained with Coomassie G250. Resulting gels were scanned at 300dpi resolution and converted into TIFF files. The intensity of protein bands was quantified using NIH ImageJ software and normalized for the

propensity of corresponding polypeptides to bind Coomassie stain, calculated based on the primary amino acid sequence according to (Compton and Jones, 1985).

DOC/Gel Filtration Chromatography Assay

The DOC treatment (Baeuerle and Baltimore, 1988) was used in combination with gel filtration chromatography to directly detect the dissociation of NF-κB dimers from IκB. To determine the conditions for our assay we tested the DOC sensitivity of endogenous IκBα (Fig. 3.6) of two *in vitro* reconstituted protein complexes (Fig. 3.6C&D). The first complex, p50:ANK(491-800), recapitulated the interactions of p50 homodimers with the C-terminal ANK domain of p105. The second complex, p52:p100CTD, represented the interactions of p52 homodimers with C-terminal domain (CTD) of p100 (a.a. 406-899) that included the ANK and death domains. The biochemical conclusions about the modes of protein interactions were drawn from a comparison of the gel filtration profiles of the identical samples in the absence and the presence of DOC, except for cytoplasmic extracts of MEF of different genetic backgrounds, which we compared with each other in presence of 0.5% DOC. Recombinant proteins were detected by Coomassie staining of PAGE gels, while endogenous proteins were detected by western blotting.

Combinatorial Calculations

The number of combinations of k elements with possible repetitions, where elements are taken from the set of n elements, equals:

MC(n,k) = (n+k-1) / (n-1)! / k! (http://mathworld.wolfram.com/Multichoose.html)

Let A and B be two set with 2 and 5 elements, respectively, representing the large and the small subunits of NF-κBsome.

Consider three types of pairs, representing RHD dimers:

I. Pairs formed by the elements of the set A. There are MC(2,2) = 3 such pairs.

II. Pairs formed by the elements of the set B. There are MC(5,2) = 15 such pairs.

III. Pairs formed by one element from A and one element from B. There are 2*5 = 10 such pairs.

Every combination of four pairs with the same total number of elements from A and from B must consist of the same number of pairs of types I and II, and a even number of pairs of type III.

There are three cases possible:

1) The 0number of pairs of types I, II, III in a combination is 0, 0, 4 respectively.

The number of such combinations is:

MC(3,0) * MC(15,0) * MC(10,4) = 1 * 1 * 715 = 715

2) The number of pairs of types I, II, III in a combination is 1, 1, 2 respectively.

The number of such combinations is:

MC(3,1) * MC(15,1) * MC(10,2) = 3 * 15 * 55 = 2475

3) The number of pairs of types I, II, III in a combination is 2, 2, 0 respectively.

The number of such combinations is:

MC(3,2) * MC(15,2) * MC(10,0) = 6 * 120 * 1 = 720

3.3. Results

3.3.1. p50 co-purifies with recombinant p105

Based on the sequence conservation between p105 and p100 in the regions encompassing protein-protein interaction domains, and on the comparable MW of endogenous p105 and p100 complexes, we hypothesized that the overall organization of p105 and p100 complexes are similar. To this end, we focused on p105:p50 complexes as a model system to study the architecture of the large p105 and p100 complexes. We noted that overexpression of p105 in HEK293T cells or in *E. coli* also yielded ~50kD polypeptides that we co-purified with p105 by affinity chromatography. These polypeptides were indeed proteolytic products of p105 because they were recognized by an antibody specific for N-terminal purification tag (Fig. 3.1, left panel) and by an antibody specific for p105/p50 (Fig. 3.1, right panel).

3.3.2. Recombinant p105 forms high molecular weight complexes with p50

Gel filtration chromatography of p105, purified from HEK293T cells, showed that p105 and its 50kD N-terminal product (which we will refer to as p50) co-elute, indicating that they interact by forming high MW complexes (Fig. 3.2). Chemical crosslinking of the p105:p50 complexes (purified from E. coli) followed by analytical gel filtration chromatography provided additional evidence that p105 and p50 interact by forming high MW complexes (Fig. 3.3). Crosslinked p105:p50 complexes eluted from the gel filtration Superose 6 column at the same volume as the native complexes did (Fig. 3.3A). SDS-PAGE analysis of gel filtration fractions and input samples, however showed that p105:p50 complexes were stably crosslinked and migrated slower then p105 or p50 polypeptides of the native complexes (Fig. 3.3B). Moreover,

the electron microscopy of negatively stained chemically crosslinked p105:p50 complexes (Fig. 3.3C) and cryoelectron microscopy of unstained crosslinked sample (Fig. 3.3D) revealed a distinct particle population.

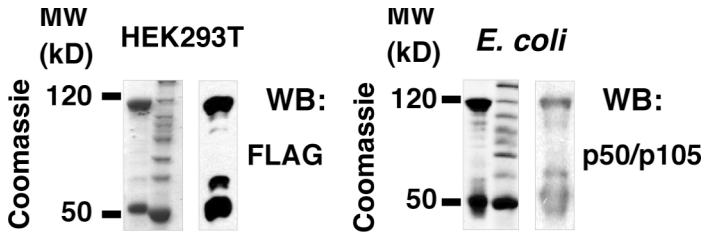

Figure 3.1 Affinity purification of recombinant p105 from mammalian and bacterial expression systems

p105 was purified by affinity chromatography from HEK293T cells (left panels) and from *E. coli* (right panel). p105 and co-purified 50kD N-terminal fragment of p105 were detected by Coomassie staining and by western blotting (WB).

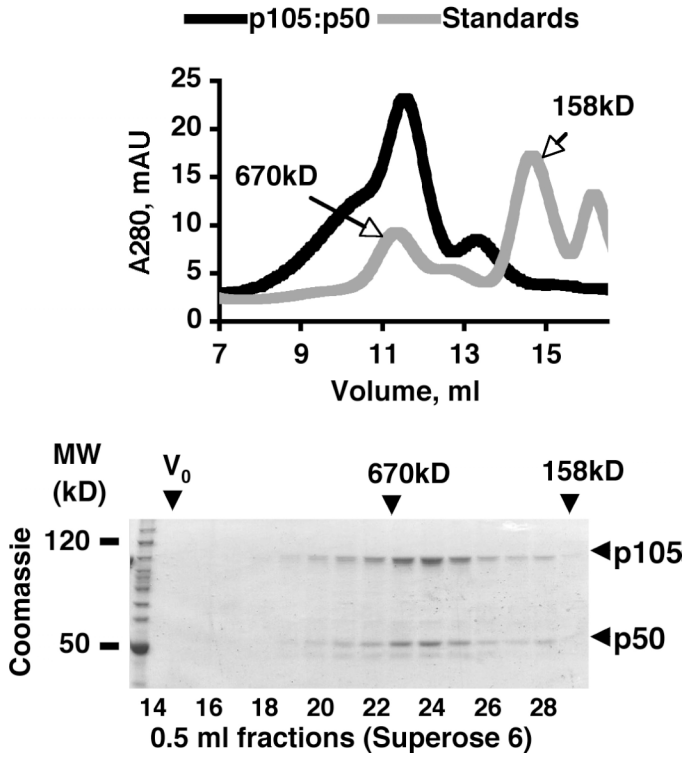

Figure 3.2 Co-purification of p50 with p105

p105:p50 (purified from HEK293T) was analyzed by gel filtration chromatography and compared to MW standards. Absorbance at 280nm (A280) was plotted against retention volume. The peaks corresponding to 670kD and 158kD MW standards are indicated by arrows (top panel). The resulting fractions we analyzed by SDS-PAGE and Coomassie staining (bottom panel).

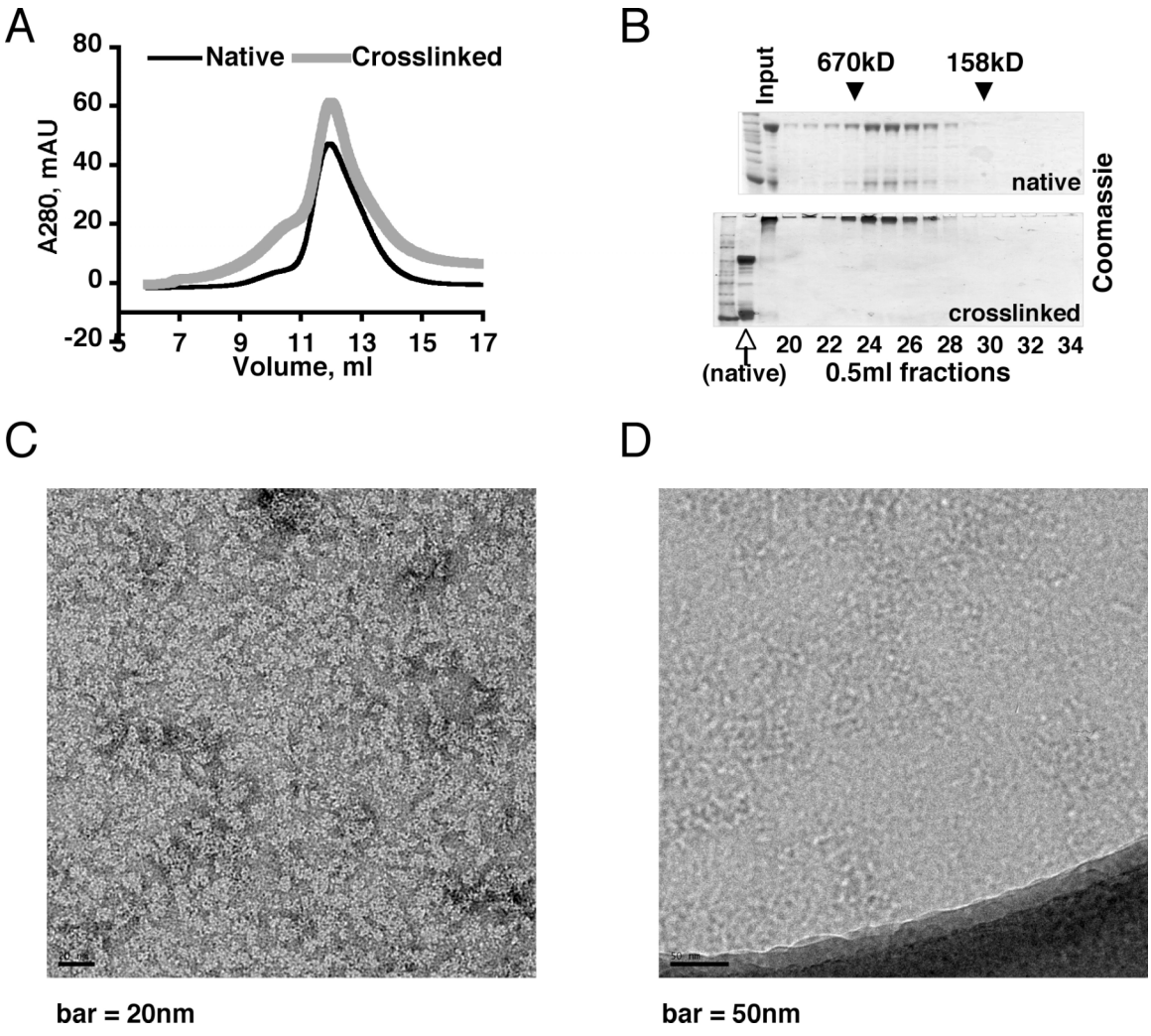

Figure 3.3 Chemical crosslinking of p105:p50 complexes

(A) Chemically crosslinked p105:p50 complexes were compared to the native p105:p50 complexes by gel filtration chromatography on a Superose 6 column. A280 was plotted against retention volume.

(B) The resulting fractions and input samples we analyzed by SDS-PAGE and Coomassie staining.

(C) Transmission electron microscopy of negatively stained chemically crosslinked p105:p50 complexes.

(D) Cryoelectron microscopy of unstained crosslinked p105:p50 complexes

3.3.3. p105 and p50 polypeptides are present in equimolar ratio in purified recombinant p105:p50 complexes

We noted that p105:p50 complexes contained approximately equal amounts of p105 and p50 polypeptides (Fig. 3.1). To quantitatively test this observation we analyzed 100μg of recombinant p105:p50 complexes by analytical gel filtration followed by SDS-PAGE and Coomassie staining (Fig 3.4 left panel). The intensity of Coomassie staining was measured and normalized for the propensity of p105 and p50 polypeptides to bind Coomassie stain (Compton and Jones, 1985). The propensity to bind Coomassie stain (binding score) was calculated based on the primary sequence of p105 and p50 polypeptides (Table 3.1). Total binding score was divided by the MW of p105 or p50 to obtain the molar stain binding coefficient (molar binding score) for each polypeptide. These coefficients were used to normalize the measured intensities of Coomassie stained protein bands. The results showed that the p105:p50 complex indeed contains equimolar amounts of both polypeptides (Fig. 3.4 right panel).

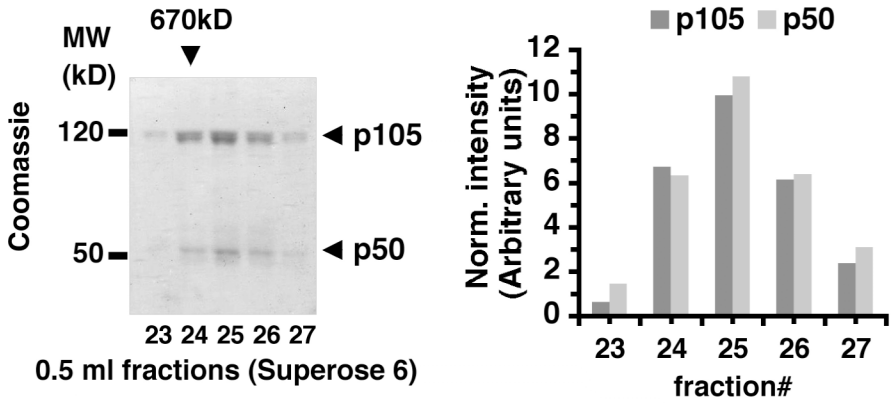

Figure 3.4 Molar ratio of p105 and p50 polypeptides in p105:p50 complex

100μg of p105:p50 complex was fractionated by gel filtration chromatography followed by SDS-PAGE and Coomassie staining (left panel). The normalized intensities of p105 and p50 bands were quantified and plotted against fraction number (right panel).

Table 3.1 Coomassie binding table

	Protein Statistics								Coomassie Binding Score	
Protein	MW, kD	Number of Amino Acids							Total Score (arbitrary units)	Molar Score = Total Score/MW (arbitrary units/mole)
		Total	Arg	Trp	Tyr	His	Phe	Lys		
His-mp105(1-971)	107.9	991	38	5	27	37	32	56	1789	16.6
His-mp50(1-430)	49.2	450	20	1	18	21	21	30	967	19.7

Amino Acid	Coomassie Binding Score (arbitrary units)
Arg	36.0
Trp	4.4
Tyr	4.7
His	4.2
Phe	1.9
Lys	1.0
All others	0

The relative propensity of each amino acid to bind Coomassie stain is reproduced from (Compton and Jones, 1985)

3.3.4. Molecular weight of bacterially expressed p105:p50 complexes

A number of methods are available to determine the molecular weight of protein in solution. Some of them are called 'absolute', which means that comparison of the sample with a material of known molecular weight is not required to calculate the result. We used Static Light Scattering (SLS) method to calculate absolute MW of recombinant p105:p50 complexes and determine that the MW of p105:p50 is indeed ~600kD (Fig. 3.5A).

The MW of bacterially expressed p105:p50 complexes was also estimated by dynamic light scattering (DLS). The MW calculated based on the measured hydrodynamic radius of p105:p50, ~9.6nm (Fig. 3.5B) was in agreement with the MW data obtained by other methods (Table 3.2).

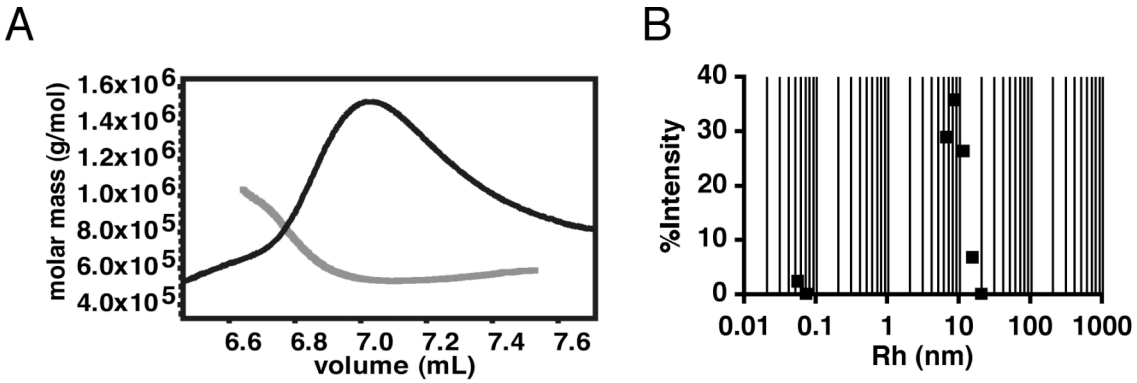

Figure 3.5 Molecular weight and hydrodynamic radius of recombinant p105:p50 complexes

(A) p105:p50 complexes purified from E. coli were analyzed by static light scattering (SLS). Calculated molar mass (grey curve) and refractive data (black curve) were plotted against retention volume.

(B) Recombinant p105:p50 complexes were analyzed by dynamic light scattering (DLS). % intensity was plotted against hydrodynamic radius, Rh.

3.3.5. Stoichiometry of p105:p50 complexes is (p105)4:(p50)4

Importantly, the MW of endogenous p105 complexes from RAW264.7 macrophages determined by gel filtration chromatography and the MW p105:p50 purified from the mammalian expression system (HEK293T cells) were in good agreement with the MW of bacterially expressed p105:p50 (Table 3.2). To obtain a stoichiometric model for p105:p50 protein complexes, we fitted the MW of p105 and p50 polypeptides (105kD and 50kD, respectively) in a 1:1 ratio into 600-660kD MW of the p105:p50 complexes, and obtained a working stoichiometric model where four p105 polypeptides interact with four p50 molecules, (p105)4:(p50)4.

Table 3.2 Molecular weight of p105 complexes

p105 complexes	source	MW, kD	method
endogenous	RAW264.7	638	GF
recombinant	HEK293T	660	GF
recombinant	*E. coli*	*616*	*GF*
		595	*SLS*
		619	*DLS*

MW of the endogenous p105 complexes and p105:p50 complexes purified from HEK293T cells were determined by gel filtration chromatography (GF). MW p105:p50 complexes purified from *E. coli* were determined by GF, static light scattering (SLS), and dynamic light scattering (DLS).

3.3.6. DOC assay

To dissect the inter-domain interactions within p105 and p100 complexes we adopted the deoxycholate (DOC) method to dissociate NF-κB from IκB. DOC was originally used to dissociate latent NF-κB activity from cytoplasmic extracts and led to the discovery of IκBα

(Baeuerle and Baltimore, 1988). Dissociation of NF-κB by this method could be monitored by NF-κB DNA binding assay. We sought a more direct method of detecting NF-κB:IκB dissociation. We performed NF-κB:IκB complexes dissociation directly on a gel filtration column and our readout of dissociation was the partitioning of complexes and individual subunits in different gel filtration fractions. We started with the assumption that DOC may disrupt the interaction between RHD domains of NF-κB dimers and ANK domain of IκB. To test this assumption, and to determine the conditions for our DOC/gel filtration assay we fractionated the endogenous IκBα (from whole-cell lysates of L929 cells) by analytical gel filtration chromatography in presence of increasing concentrations of DOC (from 0 to 1.6%). We observed that 0.2%DOC induced partial, and 0.8%DOC near complete shift in retention volume of endogenous IκBα detected by western blotting in gel filtration fractions (Fig. 3.6A). This result suggested that DOC treatment induces dissociation of endogenous IκBα:NF-κB complexes and was also consistent with the original experiments of Baeuerle & Baltimore who found that 0.4% DOC was sufficient to induce the maximal NF-κB DNA binding activity from cytoplasmic extracts (Baeuerle and Baltimore, 1988).

We also tested whether interactions of p105 and p100 C-terminal ANK domains with NF-κB RHD dimers are DOC sensitive. To this end we used two protein complexes reconstituted from N- and C-terminal polypeptides of p105 and p100. p50:ANK(491-800) was reconstituted in vitro from p50 homodimers and C-terminal fragment of p105 (a.a. 491-800) that contained ANK domain. p52:p100CTD was reconstituted from p52 homodimers and C-terminal fragment of p100 (a.a. 406-899) that included ANK and death domains. Both of these complexes dissociated in presence of DOC in gel filtration buffer, proving that ANK domains of p105 and p100 bind NF-κB dimers in DOC-sensitive manner (Fig. 3.6B&C).

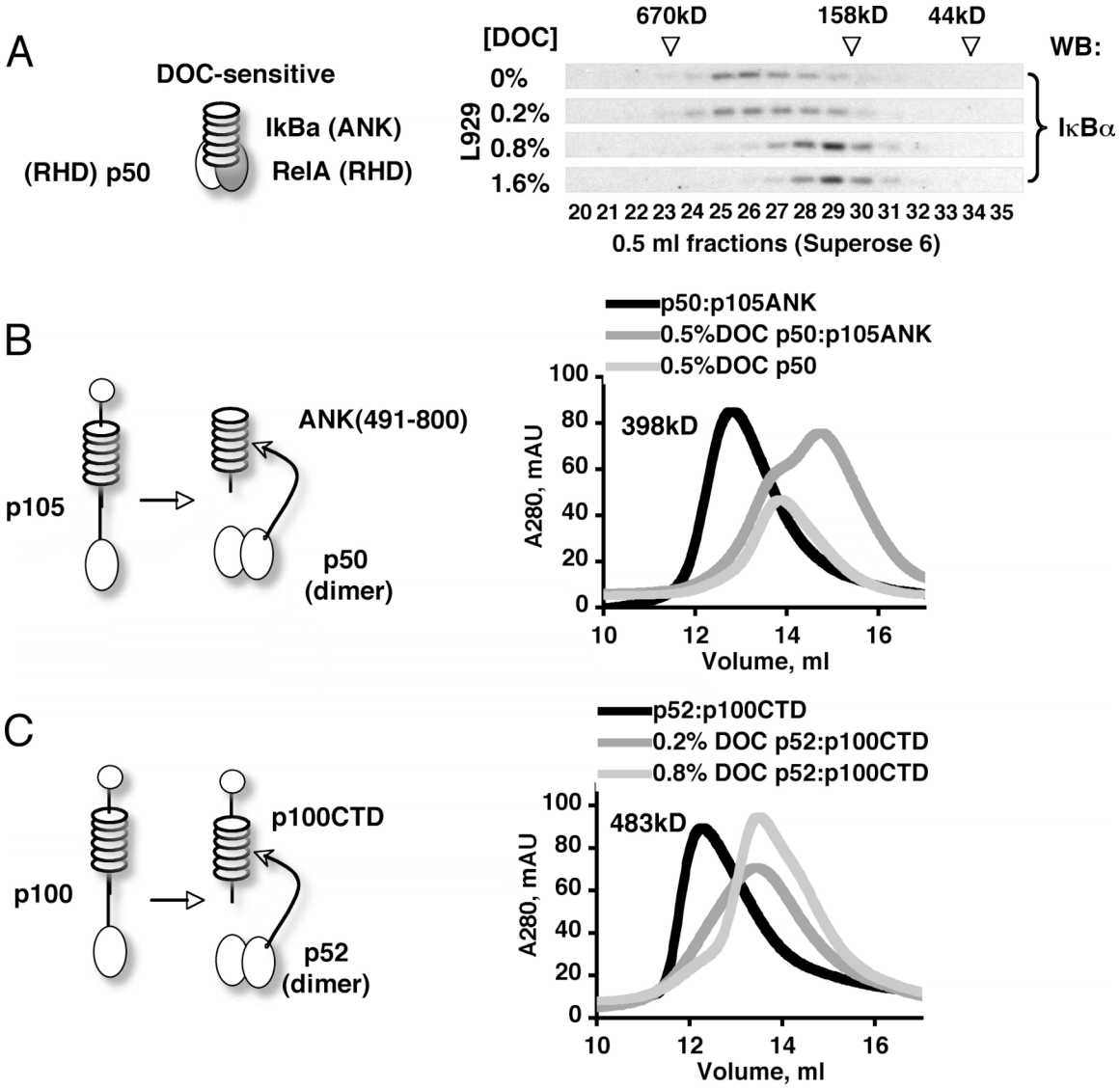

Figure 3.6 DOC assay tests the interactions of ANK domains with RHD dimers

(A) Effect of DOC on endogenous IκBα complexes from L929 cell lysates. Whole cell lysates were prepared and analyzed by gel filtration (GF) chromatography. IκBa was detected in the indicated fractions by western blotting (WB).

(B) Complete dissociation of p50:ANK(491-800) complexes in the presence of 0.5% DOC determined was detected by gel filtration chromatography on a Superose 6 analytical column. A280 was plotted against retention volume. The MW of the native p50:ANK(491-800) complex is indicated.

(C) Dissociating effect of the increasing concentrations of DOC on p52:p100CTD(406-899) complex was determined by gel GF on a Superose 6 analytical column. A280 was plotted against retention volume. The MW of the native p52:p100CTD complex is indicated.

3.3.7. Two types of inter-domain interactions within p105 and p100 complexes with NF-κB subunits

Because p105 and p100 proteins contain RHD and ANK domains, there are at least two types of inter-domain interactions that can be simultaneously utilized in the assembly of the high MW p105 and p100 complexes with other NF-κB subunits. The first type constitutes the individual NF-κB subunits binding to the N-terminal RHD domains of p105 and p100 (Fig. 3.7, left panel). This type of interactions was suggested by the pioneering study of the p105 protein by Rice and colleagues (Rice et al., 1992). In addition, the "pre-assembled" NF-κB dimers can bind to the ANK domains of p105 and p100 (Fig. 3.7, right panel), as was shown for the p100 protein by Basak et al. (Basak et al., 2007). To obtain clear experimental evidence in support of the "dual binding mode" hypothesis we used our combined DOC/gel filtration chromatography assay. We analyzed the recombinant p105:p50 complexes and found that approximately half of the p50 dissociated from p105 even at the lowest (0.2%) concentration of DOC (and was detected in lower MW fractions), while some p50 remained bound to p105 at the highest (1.6%) concentration of DOC (Fig. 3.7B). Based on these observations we concluded that both modes of binding indeed are involved in the assembly of the recombinant p105:p50 complexes.

To find what types of interactions are involved in the assembly of p105 with RelA NF-κB subunit, we tested the DOC-sensitivity of the recombinant p105:p50:RelA(19-304) complexes. p105:p50:RelA(19-304) complexes were purified from *E. coli* after coexpression of p105 and RelA(19-304), where the latter protein corresponds to RHD of RelA. RelA(19-304) was stably incorporated into high MW complexes with p105:p50 in a standard gel filtration conditions (Fig. 3.8, left panel). In 0.8% DOC-containing buffer, however, we observed that both p50 and RelA(19-304) partially dissociated from p105, and were detected in high and in low MW fractions (Fig. 3.8, right panel). We concluded that both proteins, p50 and RelA, utilize two

modes of binding to p105 (though RHD and ANK domains). RelA, however, was preferentially bound to RHD of p105 when two proteins were co-expressed in *E. coli*.

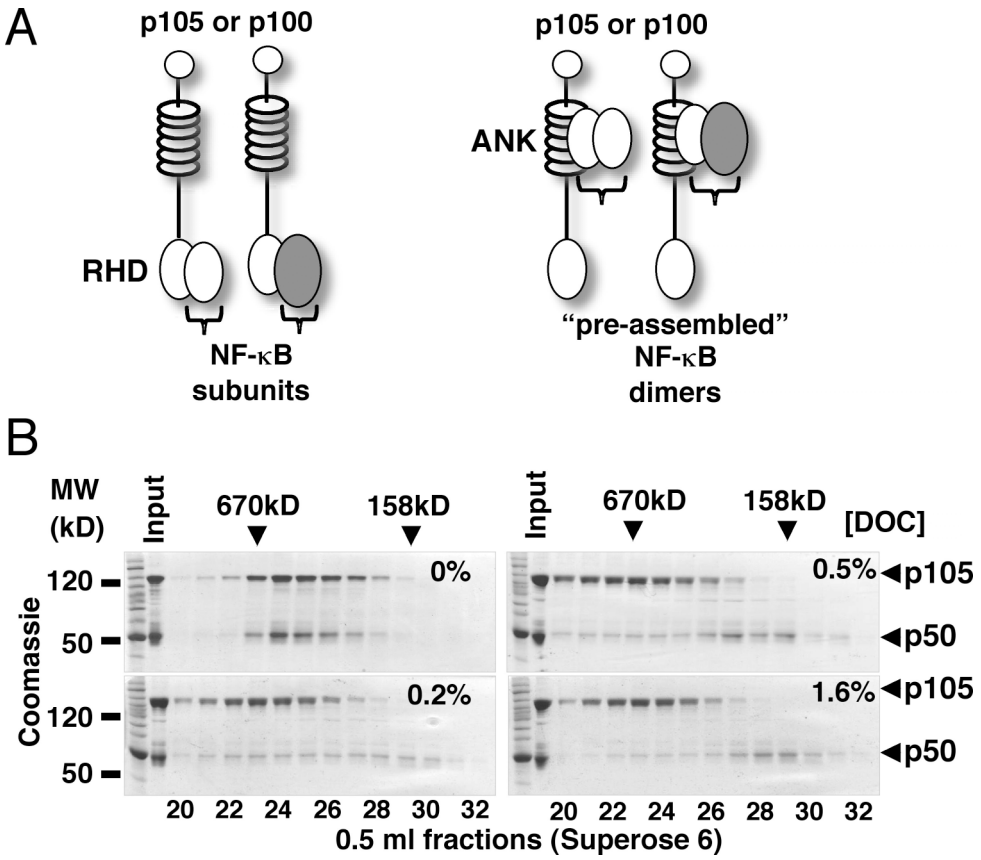

Figure 3.7 Two modes of binding of p50 NF-κB subunits to p105

(A) Individual NF-κB subunits interact with p105 and p100 via dimerization of RHD domains (left panel); "pre-assembled" NF-κB dimers interact with p105 or p100 ANK domains (right panel).

(B) Recombinant p105:p50 complexes were analyzed by gel filtration chromatography in the presence of 0-1.6% of sodium deoxycholate (DOC) followed by SDS-PAGE and Coomassie staining.

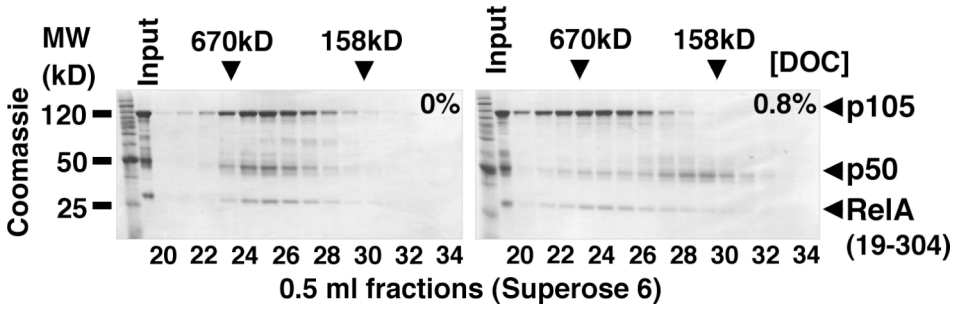

Figure 3.8 Two modes of binding of RelA to p105

Recombinant p105:p50:RelA(19-304) complexes were analyzed by gel filtration chromatography in standard conditions and in the presence of 0.8% DOC followed by SDS-PAGE and Coomassie staining.

To test how endogenous p50 and p52 proteins interact with p105 and p100 we fractionated the cytoplasmic extract of THP-1 cells by gel filtration chromatography in the presence and in the absence of DOC and analyzed the resulting fractions by western blotting with antibodies specific for p52/p100 (Fig. 3.9, top panels), p50/p105 (Fig. 3.9, middle panels) and IκBα (Fig. 3.9, bottom panels). DOC treatment caused complete dissociation of IκBα complexes thus providing a positive control for the effectiveness of DOC treatment of cytoplasmic extracts in combination with gel filtration chromatography (Fig. 3.9, bottom panels). DOC treatment, however, caused only partial dissociation of p52 from the high MW complexes (Fig. 3.9, top panels). We concluded that p52 utilizes both binding modes to interact with p105 and/or p100 in high MW. The dissociation of p50 from high MW complexes was more difficult to establish because p50 is detected in the lower MW fractions even before DOC treatment (Fig. 3.9, middle panels). The retention of p50 in high MW gel filtration fractions (coincident with p105 and p100) in the presence of 0.5%DOC, however, was clearly observed, providing evidence of the direct interaction of endogenous p50 subunits with the RHD of p105 and/or p100.

To test if the endogenous RelA subunits also utilize a dimerization interface in RHD to incorporate into high MW p105 and/or p100 complexes, we fractionated the cytoplasmic extracts of *ikba-/-,ikbb-/-,ikbe-/-* MEF in the presence of 0.5%DOC and compared gel filtration profiles to wt MEF, and to *nfkb1-/-,nfkb2-/-* MEF, deficient for both p105 and p100. More RelA was detected in high MW fractions of cytoplasmic extracts from *ikba-/-,ikbb-/-,ikbe-/-* cells (deficient for IκBα, IκBβ, and IκBε) compared to fractionated cytoplasmic extracts of wt or *nfkb1-/-,nfkb2-/-* MEF (Fig. 3.10). This result confirmed that endogenous p105 and p100 could interact with RelA by direct dimerization of their RHD domains.

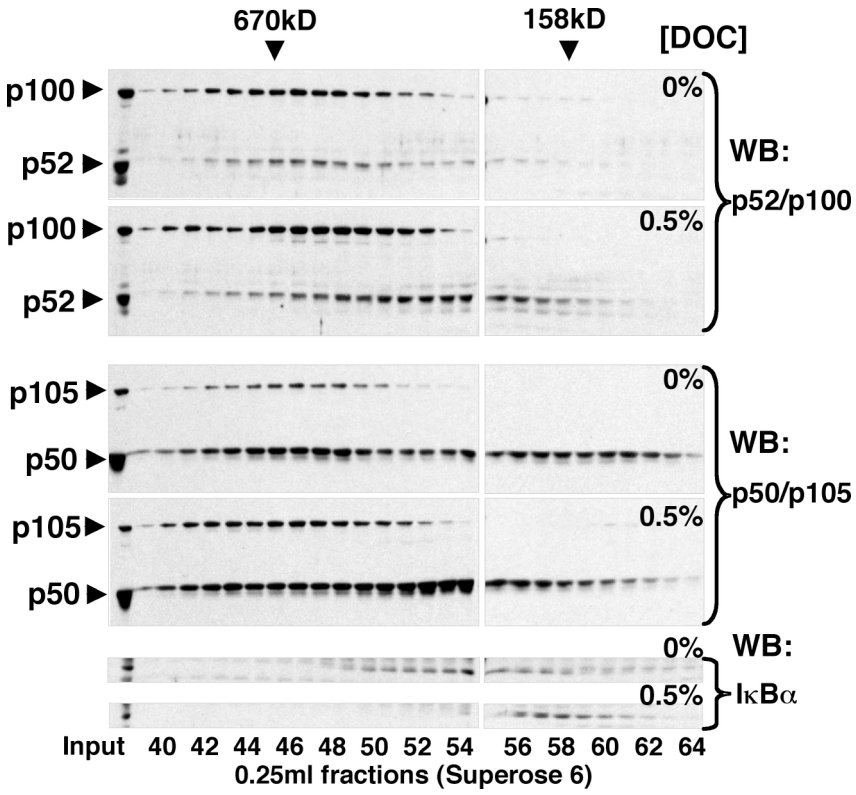

Figure 3.9 Two modes of binding of endogenous NF-κB subunits to p105 and/or p100

Cytoplasmic extracts of THP-1 cells were analyzed by gel filtration chromatography in standard conditions and in the presence of 0.5% DOC followed by western blotting (WB) to detect p100/p52 (top panels), p105/p52 (middle panels), and IκBα (bottom panels).

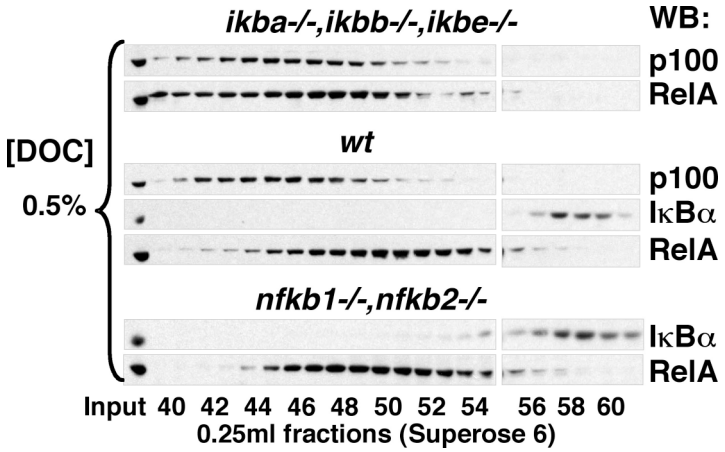

Figure 3.10 Endogenous RelA utilizes RHD domain to bind to p105 and/or p100

Cytoplasmic extracts of *ikba-/-,ikb-/-,ikbe-/-* (top panels); wild type (wt, middle panels); and *nfkb1-/-,nfkb2-/-* (bottom panels) mouse embryonic fibroblasts were analyzed by gel filtration chromatography in the presence of 0.5% DOC. p100, IκBα, and RelA were detected by western blotting (WB).

In all, the results of our DOC experiments demonstrated that NF-κB subunits do, indeed, utilize two modes of binding to p105 and p100: 1) direct binding to p105 or p100 RHD, and 2) binding to p105 and p100 ANK domain as constituents of NF-κB dimers (Fig. 3.7A).

3.3.8. Evolutionary conserved oligomerization "domain" of p105 and p100

We noted that, in contrast to isolated RHD domains, which form dimers in solution (Chen et al., 1999), the isolated C-terminal fragments of p105 and p100 (p105CTD and p100CTD, respectively) are oligomeric in solution. The MW of these fragments, determined by gel filtration chromatography, was at least three times greater than the theoretical MW of their corresponding monomers (Fig. 3.11). Based on this evidence, we suspected that full-length p105 and p100 proteins also oligomerize *via* C-terminal regions.

To identify the putative oligomerization domain(s) we analyzed the conservation of p105 and p100 protein sequences. We performed a pairwise alignment of the translated protein sequences derived from each pair of the homologous exons from *NFKB1* and *NFKB2* genes (Fig. 3.12). We focused on the conserved C-terminal regions of p105.

First, we experimentally tested if the C-terminal death domain contributed to the oligomerization of p105. We purified the p105 mutant protein that lacks a death domain, p105(1-800), and compared it to the full-length p105 by gel filtration chromatography. We found that p105(1-800) (MWmono88kD) forms high MW complexes similar to full-length p105 (Fig. 3.13). We, therefore, concluded that a death domain is not required for the oligomerization of p105. This result was further supported by the observation that the C-terminal p105 fragment, ANK(491-800), which also lacked a death domain, formed a high MW (398kD) complex with p50 (Fig. 3.6C).

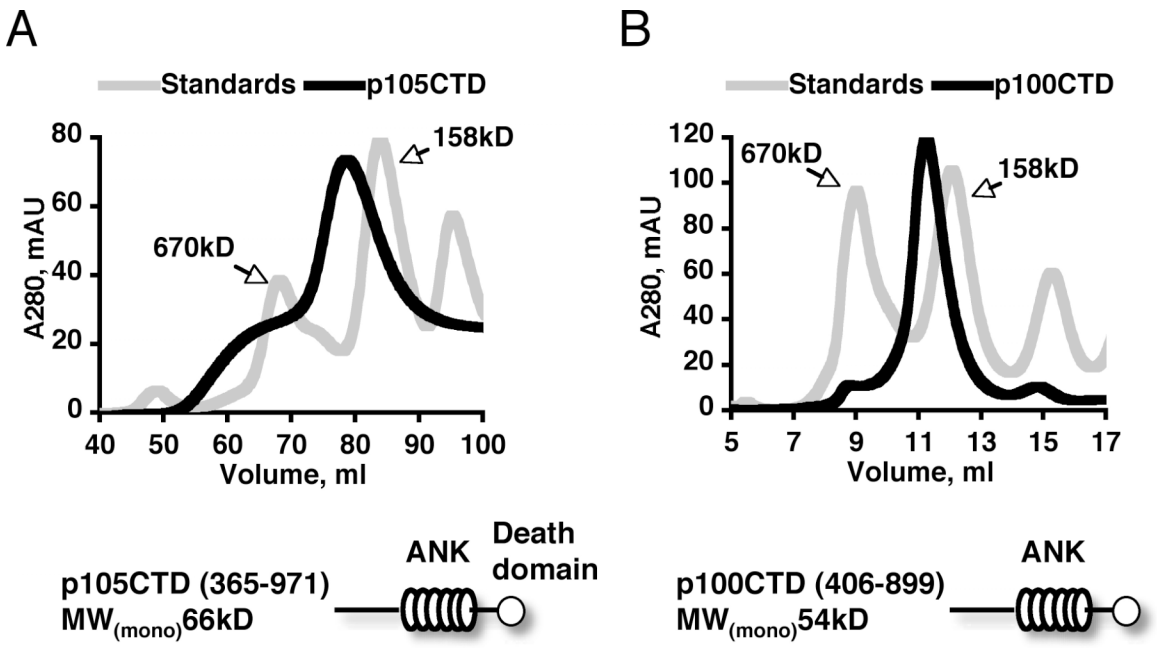

Figure 3.11 Recombinant C-terminal polypeptides of p105 and p100 are oligomeric

(A) Isolated C-terminal fragment of human p105 protein (p105CTD, amino acids 368-969, purified from Sf9 insect cells) was analyzed by gel filtration chromatography on a preparative Superdex 200 column and compared to MW standards. Absorbance at 280nm (A280) was plotted against retention volume. The peaks corresponding to 670kD and 158kD MW standards are indicated. The domain organization and the MW of monomeric p105CTD fragment are also shown.

(B) Isolated C-terminal fragment of human p100 protein (p100CTD, amino acids 406-899, purified from *E. coli*) was analyzed by gel filtration chromatography on an analytical Superdex 200 column and compared to MW standards. A280 was plotted against retention volume. The peaks corresponding to 670kD and 158kD MW standards are indicated. The domain organization and the MW of monomeric p105CTD fragment are shown.

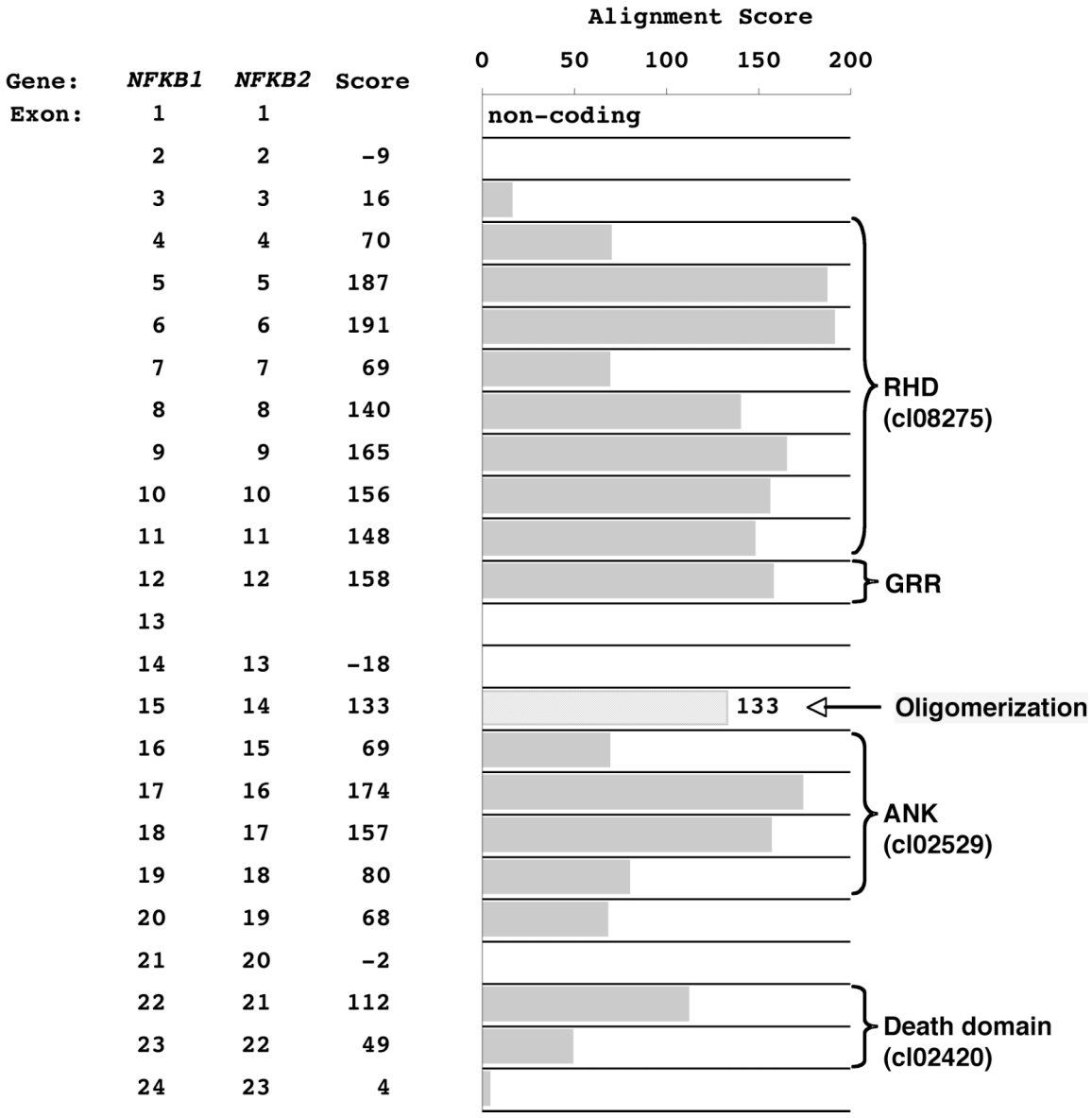

Figure 3.12 p105 and p100 sequence conservation

Pairwise alignment of the translated protein sequences derived from the homologous exons of human *NFKB1* and *NFKB2* genes were performed using the sequence alignment tool CLUSTAL W (Thompson et al., 1994). The alignment scores were plotted against *NFKB1* exon number. The numbers for corresponding homologous exons of *NFKB2* gene and the numeric values for the alignment scores are also given. Conserved protein domains (according to NCBI domain classification, with corresponding accession numbers) and glycine rich region (GRR) are indicated with brackets next to the alignment score bar graph. Arrow points to the region (highlighted in the bar graph with light-grey color, score=133) that can serve as oligomerization determinant for p105 and p100 (as we determined in this study).

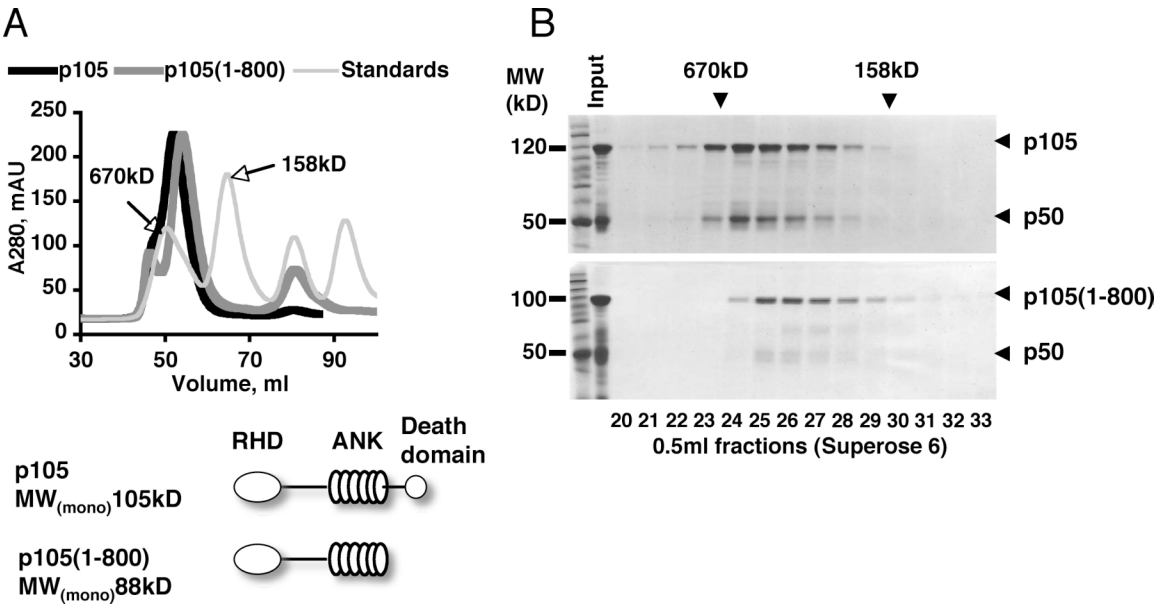

Figure 3.13 Death domain is not required for p105 oligomerization

(A) Full-length p105 protein and p105 mutant protein that lacks the C-terminal death domain were purified from E. coli and analyzed by gel filtration chromatography. A280 was plotted against retention volume. The peaks corresponding to 670kD and 158kD MW standards are indicated. The domain organization and the theoretical MW of monomeric proteins are also shown.

(B) Gel filtration fractions from the experiment shown in A were analyzed by SDS-PAGE and Coomassie staining.

Of the remaining regions of p105, under our consideration, the protein sequences immediately preceding the ANK domains displayed the highest degree of conservation (Fig. 3.12). To test if this conserved sequence feature could function as an oligomerization determinant we compared two recombinant C-terminal fragments of p105, which either included or lacked the conserved sequence immediately preceding ANK, by gel filtration chromatography at two different concentrations. A concentration–dependent shift in the retention volume of the ANK(491-800) fragment, containing the conserved sequence, indicated that this protein oligomerized in a concentration-dependent manner (Fig. 3.14A), while the p105 fragment lacking

the conserved sequence, ANK(531-811) did not (Fig. 3.14B). Interestingly, Beinke and colleagues have suggested that the same p105 region contributes to the dimerization of p105 (Beinke et al., 2003). They concluded this based on the results of the comparative biophysical analysis of similar p105 ANK domain-containing fragments that we also used in this study.

To test if ANK(491-800) polypeptide can interact with p105 we mixed the purified p105:p50 complexes with ANK(491-800) *in vitro* and followed with gel filtration chromatography. We observed a reduction of the MW of p105:p50 assembly and the apparent incorporation of ANK(491-800) into p105:p50 complexes (Fig. 3.15). As a control for the specificity of this interaction we used the mixture of p105:p50 complexes with the non-oligomerizing ANK(531-811) polypeptide and observed that ANK(531-811) neither reduced the MW of nor incorporated into p105:p50 complex (Fig. 3.15). Thus, we concluded that ANK(491-800) interacted with p105 through the conserved oligomerization sequence preceding the ANK domain.

In all, our results showed that the evolutionarily conserved region with predicted helical structure preceding the ANK domain in the p105 and p100 proteins (corresponding to a.a. 503-530 of the mouse p105) can serve as an oligomerization determinant of p105 and p100 proteins (Fig. 3.16).

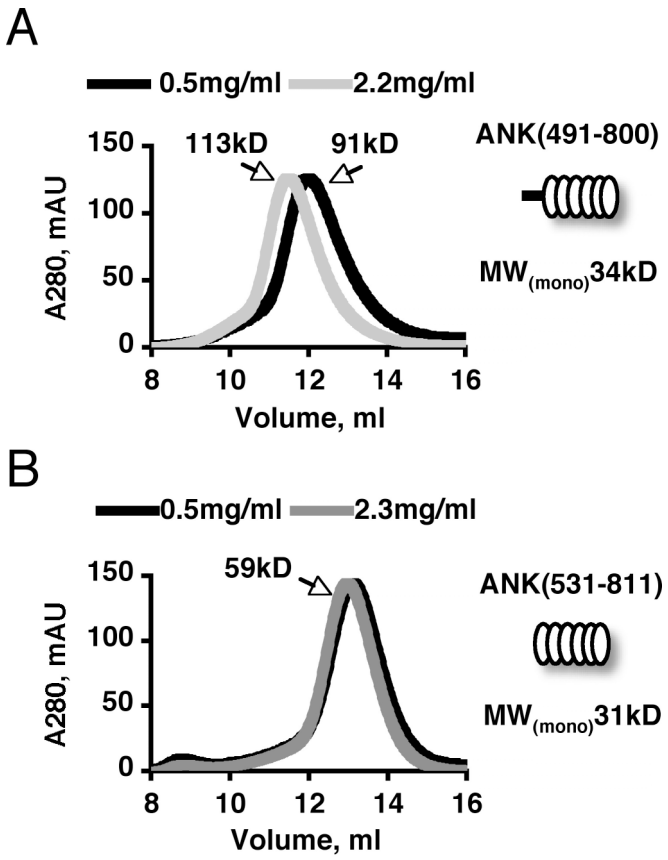

Figure 3.14 Identification of the conserved oligomerization "domain" in the C-terminal region of p105

(A-B) Purified p105 fragments, ANK(491-800) (A) and ANK(531-811) (B) were analyzed by gel filtration chromatography (GF) at two concentrations. Normalized absorbance at 280nm (A280) was plotted against retention volume. The MW of p105 fragments (determined by GF) are indicated. Schematic drawings of the p105 fragments and their corresponding monomeric MW are shown.

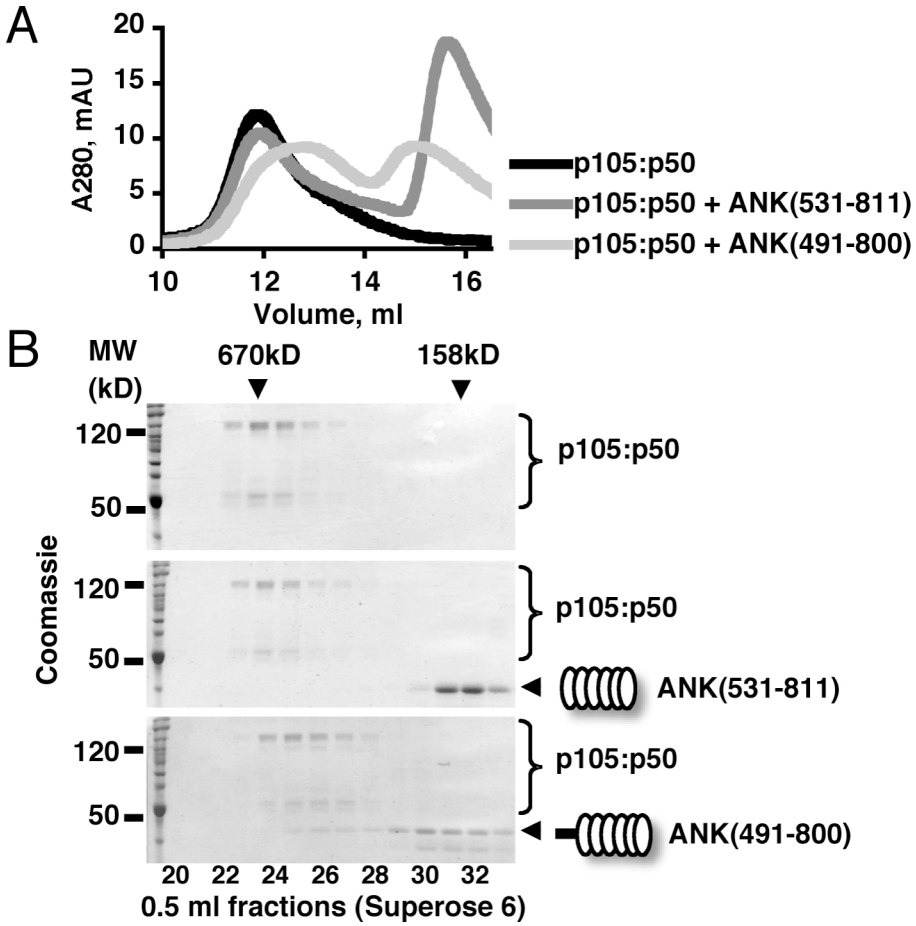

Figure 3.15 Interaction of the conserved oligomerization "domain" with p105 complex

(A-B) Purified p105 fragments, ANK(531-811) and ANK(491-800), were mixed with recombinant p105:p50 complex *in vitro*, and resolved by GF. A280 was plotted against retention volume (A). Resulting fraction were analyzed SDS-PAGE followed by Coomassie staining (B).

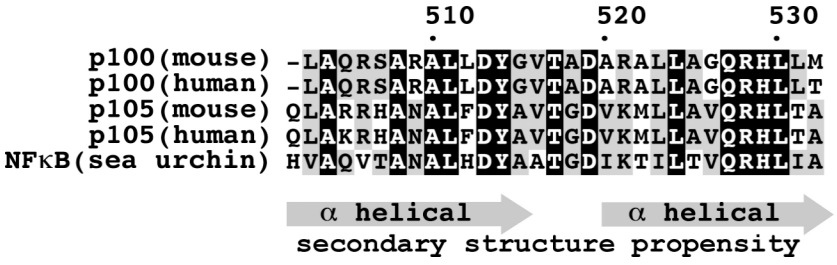

Figure 3.16 Sequence alignment of oligomerization "domain" from p105 and p100

3.4. Discussion

The architecture of p105 and p100 is evolutionarily conserved

p105 and p100 are homologous proteins. Their RHD and ANK domains are also similar to classical NF-κB and IκB, respectively. We constructed two phylogenetic trees based on sequence alignments of RHD and ANK domains of human p105 and p100 proteins with other human IκB and NF-κB proteins and with evolutionarily distant orthologs of p105 and p100 (Fig. 3.17). The alignments of RHD and ANK domains showed that human p105 and p100 proteins are more similar to their ancient multi-domain orthologs from sea urchin and sea squid than to classical single-domain, NF-κB and IκB proteins. This suggests that the multi-domain organization of p105 and p100 was preserved during evolution.

The oligomerization determinant in the C-terminal half of p105 is also an evolutionarily conserved region in p105 and p100 proteins, encoded by a separate exon (Fig. 3.12 & Fig. 3.16). We hypothesize that oligomerization of p105 and p100, which brings several NF-κB subunits into close proximity, may facilitate their stable binding within a complex. We were unable to detect NF-κB "subunit exchange" between stable oligomeric p105:p50 complexes and RelA(19-304) homodimers (Fig. 3.18). This negative observation supports our hypothesis because, in contrast, the subunit exchange between simple dimeric p50:p50 complexes and RelA homodimers readily occurs *in vitro* (Chen et al., 1999) and is discussed in the literature as a potential mechanism of NF-κB biogenesis (Hoffmann et al., 2006).

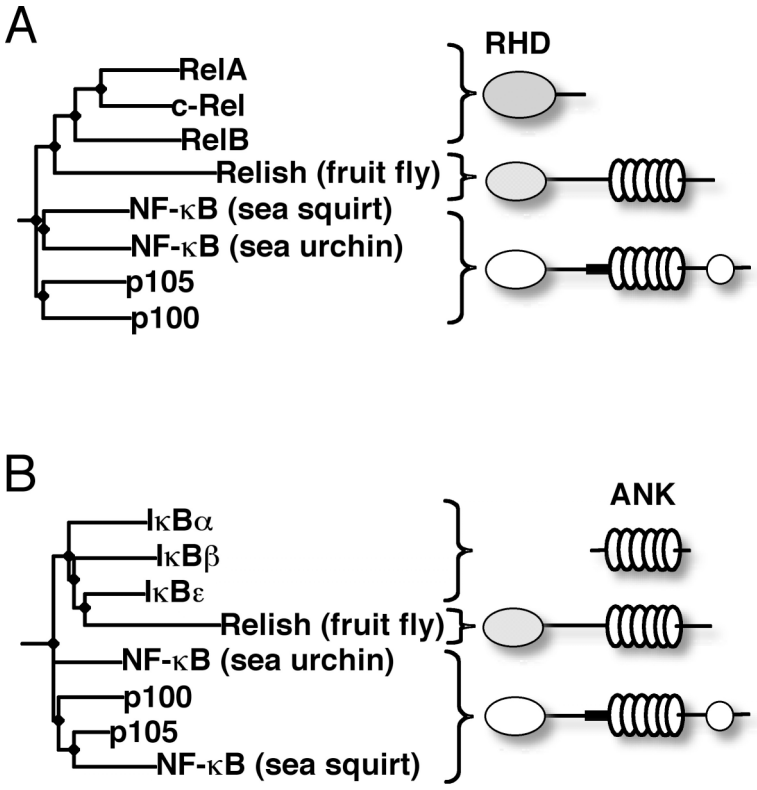

Figure 3.17 Multi-domain organization of p105 and p100 is evolutionarily conserved

(A-B) Rooted phylogenetic trees were constructed based on the sequence alignments (Felsenstein, 1989) of RHD domains (A) and ANK domains (B) from human IκB and NF-κB proteins and from p105/p100 orthologs from fruit fly (*D. melanogaster*), sea urchin (*S. purpuratus*), and sea squirt (*C. intestinalis*). The domain organization of proteins used for the sequence alignments are shown.

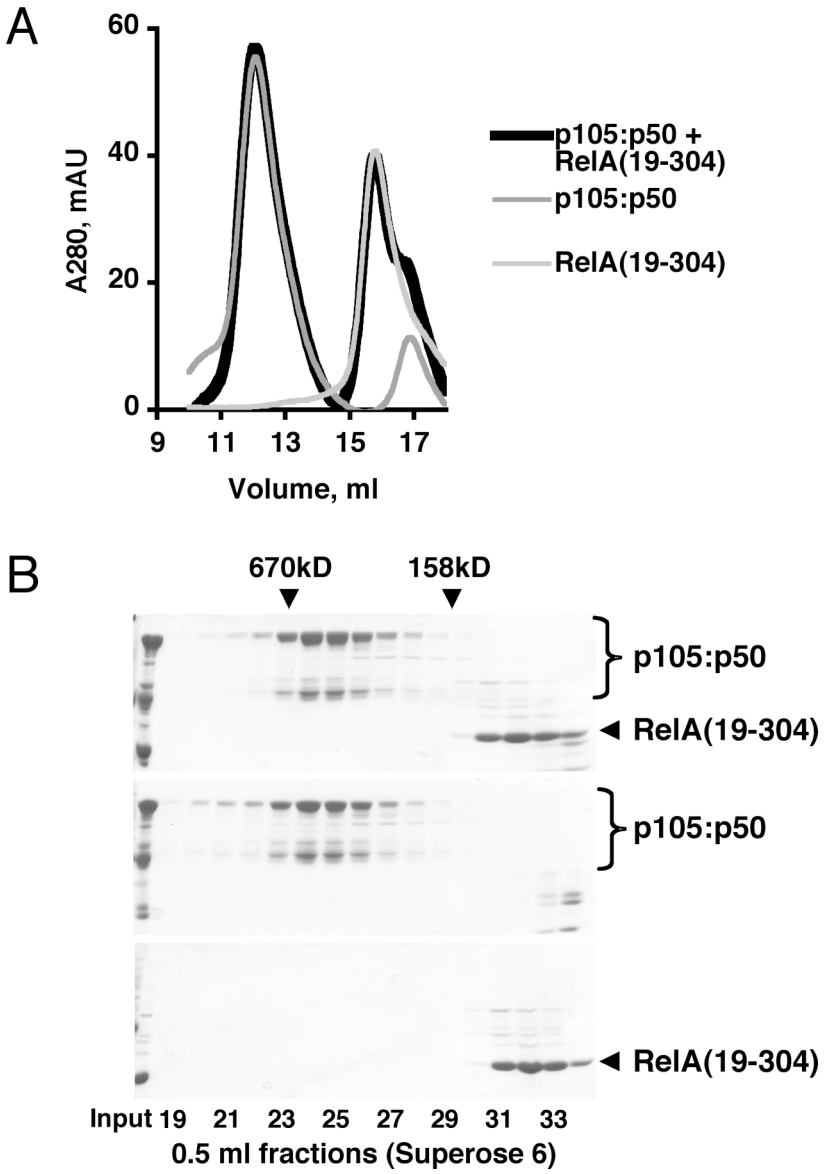

Figure 3.18 Subunit exchange between RelA RHD homodimers and p105:p50 complexes is not detected

(A) Subunit exchange between RelA RHD homodimers, RelA(19-304), and p105:p50 complexes was tested by gel filtration chromatography on an analytical Superose 6 column. A280 was plotted against retention volume.

(B) Gel filtration fractions from the experiment shown in (A) were analyzed by SDS-PAGE followed by Coomassie staining. No RelA(19-304) incorporation in p105:p50 complex was detected (top panel).

Stoichiometric model for p105 and p100 complexes

p105 and p100 are multi-domain, "modular" proteins. The complexity of interactions of p105 and p100 with other NF-κB subunits has been long appreciated, and has given rise to several models for the p105 and p100-containing complexes (Basak et al., 2007; Mercurio et al., 1993; Rice et al., 1992).

In this study we showed that: 1) p105 and p100 form high MW complexes with other NF-κB subunits; 2) these complexes are heterogeneous in composition; 3) the highly pure recombinant p105:p50 complexes contain an equimolar amount of large and small subunits in 4:4 stoichiometry, (p105)4:(p50)4. We experimentally tested three types of interactions that are involved in the formation of the high MW p105 and/or p100 complexes: 1) C-terminal oligomerization; 2) dimerization of RHD domains; and 3) binding of RHD dimers to ANK domains of p105 and p100. Here we propose that, utilizing these three types of interactions, p105 and p100 assemble in a 1:1 ratio with other NF-κB subunits in a combinatorial manner giving rise to a finite number of complexes, for which we coined the term NF-κBsomes (Fig. 3.19).

Our model provides a unifying extension of previously published models. The complexes pictured in the left panel of Figure 3.19C, for example, can be described as tetramers of "self-inhibited dimers" originally envisioned by Rice et al. (Rice et al., 1992); the right panel in the same figure corresponds to a dimer of the "IκB delta" complex proposed by Basak et al. (Basak et al., 2007); while the middle cartoon represents the combination of the two models.

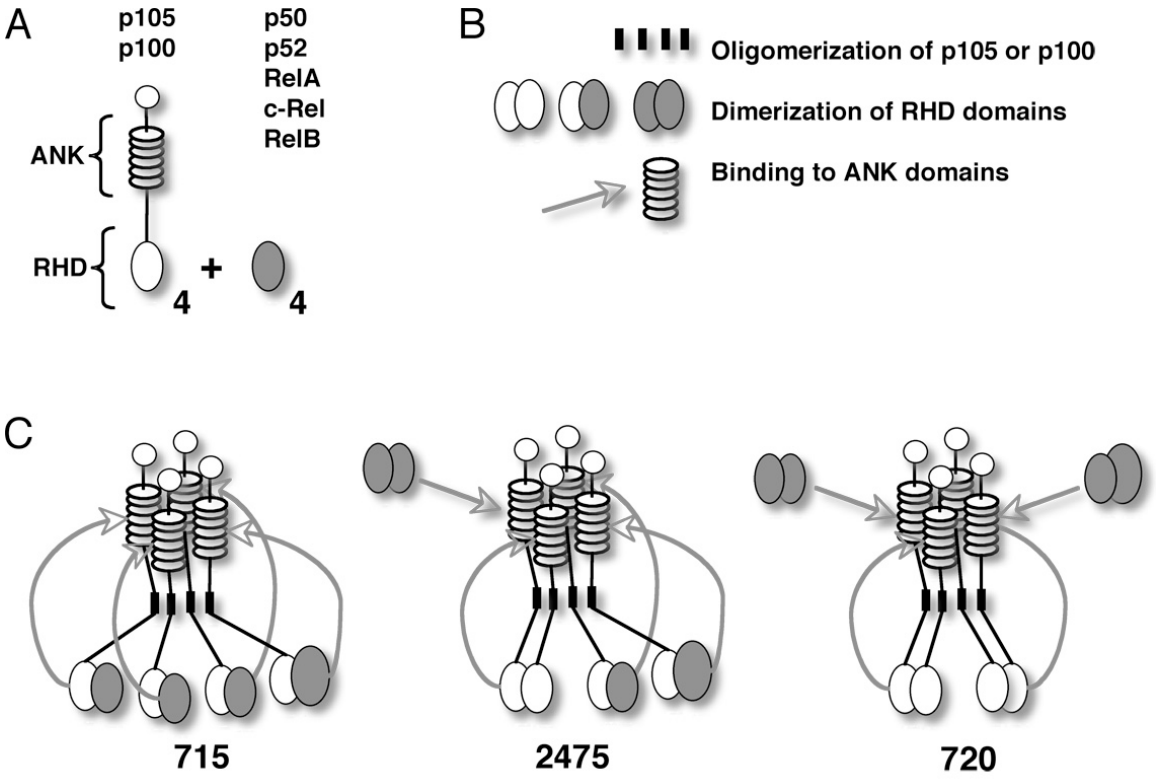

Figure 3.19 Stoichiometric model for p105 and p100 complexes

(A) Stoichiometric components of the p105 and p100 complexes.

(B) The protein-protein interactions within the p105 and p100 complexes.

(C) Three classes of arrangements of the components of the p105 and p100 complexes and the theoretical combinatorial numbers of the individual sub-types within each class calculated based on the experimentally determined stoichiometric model (unrestricted to the subunit binding specificities).

Theoretical number for each of the three possible “types” of arrangements of p105/p100 with other NF-κB subunits (shown in Fig. 3.19C) was calculated by computing the number of "combinations with repetition" operating on two sets of elements (representing the “large”, p105, p100; and the “small”, RelA, c-Rel, RelB, p50, and p52, subunits of the complex, Fig. 3.19A). For this calculation we applied two biochemically sound restrictions determined during our current investigation: 1) every combination (complex) consists of four pairs of elements (pairs

represent RHD dimers); and, 2) every combination contains the same total number of elements from each set (the set of "large" and the set of "small" subunits). The results illustrate the high degree of compositional heterogeneity within a pool of "NF-κBsomes".

We have not yet determined whether the predicted helical oligomerization regions of p105 or p100 assume a parallel or anti-parallel orientation (Fig. 3.19C shows a parallel orientation). We expect, however, that our model will perform for any orientation of oligomerization "domains" because each p105 and p100 molecule contains the conserved glycine rich region (GRR), which encompasses at least 50 amino acids, and is located between the RHD domain and the oligomerization region. The low structural complexity of GRR can provide p105 and p100 sufficient structural flexibility to accommodate intra-molecular interactions in any orientation of their oligomerization "domains". It should be emphasized, therefore, that our model recapitulates all other biochemical aspects of the p105 and p100 complexes that we experimentally determined here: the compositional heterogeneity, high MW, subunit stoichiometry, and inter-domain interactions found within these complexes.

3.5. Chapter 3 acknowledgements

I thank Johanne Le Coq for her help with static light scattering experiments; Erika Mathes for valuable discussions and for purified RelA RHD protein; Max Alekseyev for combinatorial calculations; Timothy Baker and Norman Olson for theoretical and practical training in electron microscopy; Kristin Parent for her substantial help with cryoelectron microscopy of p105:p50 complexes. I acknowledge the use of the UCSD Cryo-Electron Microscopy Facility, which is supported by NIH grants 1S10RR20016 and GM033050 to Dr. Timothy S. Baker and a gift from the Agouron Institute to UCSD.

Chapter 3 has been submitted for publication of the material as it may appear in Molecular Cell, 2009. Savinova, Olga V.; Ghosh, Gourisankar. "p105 and p100 NF-κB precursors function as a core of multi-protein heterogeneous NF-κBsomes". The dissertation author was the primary investigator and author of this paper.

Chapter 4

p105 and p100 processing

4.1. Introduction

p105 and p100 function as the precursors of NF-κB subunits p50 and p52 and as inhibitors of NF-κB signaling (Beinke and Ley, 2004). In addition, p105 is essential for the regulation of extracellular signal-regulated kinase (ERK) signaling downstream of multiple Toll like receptors (Banerjee et al., 2006). Each of these functions of p105 and p100 requires their regulated proteolysis by a multiprotein cellular protease, the proteasome (Beinke and Ley, 2004).

The mechanism of p105 processing that generates p50 NF-κB subunit was first addressed in early 1990s after the discovery that the gene coding for p50 NF-κB subunit has an open reading frame corresponding to the much larger protein, p105 (Ghosh et al., 1990; Kieran et al., 1990). Thus, Fan and Maniatis have determined that *in vitro* translated p105 could be processed to p50 by the cytosolic protease from HeLa cells in ATP dependent manner (Fan and Maniatis, 1991). They also mapped the site of p105 processing (~ amino acid 435 of human sequence) and determined that the C-terminal portion of p105 (containing ANK domain) is completely degraded as a result of this proteolytic event. The later study from the same laboratory established that proteasome activity is required for p105 processing (Palombella et al., 1994). They used specific inhibitors for proteasome and yeast strains deficient in proteasome subunits to test the function of this enzymatic activity in p105 processing. In the same study, however, researchers noted that neither 20S nor 26S proteasome, although required, is sufficient to proteolyse *in vitro* translated p105 fragment containing the processing site.

Upon overexpression in mammalian cells, p100 processed at least ten fold less efficiently compared to p105 under the same conditions. (Heusch et al., 1999). The ineffective processing of

p100 appears to be either "encoded" by its C-terminal regions/domains or by the processing site itself. Replacment of the C-terminal half of p100 (including processing site) with the equivalent sequences from p105 enhanced p52 generation (Heusch et al., 1999). The reciprocal experiments showed that p50 generation, in turn, could be inhibited by "swapping" of p105 processing site and C-terminal half with the corresponding regions from p100 protein (Heusch et al., 1999).

The first experimental evidence that p105 and p100 proteolysis might be regulated came from the studies of p105 and p100 processing in the presence of ectopically expressed kinases. Accordingly, NF-κB inducing kinase (NIK) (Xiao et al., 2001) or tumor progression 2 (Tpl2) (Belich et al., 1999) stimulate p100 and p105 processing, respectively. Moreover, overexpression of IKK2 has also been shown to stimulate p105 proteolysis (Orian et al., 2000). Studies concerning the regulation of p105 and p100 procession, however, are challenging due to the lack of the reliable "processing assay". Metabolic pulse-chase experiments remain the golden standard to assay the NF-κB precursor/product relationship. As an alternative, the change in the ratio between precursor, p105 or p100, and the corresponding product, p50 or p52 (detected by western blotting of cell lysates), was also used as readout of processing. The results from this latter approach are more difficult to interpret because the precursor/product ratio depends on several other factors in addition to the kinetics of processing. These factors include the rates of synthesis and degradation of p105 and p100 as well as the rates of degradation or subcellular re-localization of their corresponding processed products. The magnitude of these other parameters are known to be affected by cellular conditions in several ways: i) stimuli that induce NF-κB activation are also enhance p105 and p100 synthesis due to the presence of NF-κB response elements in their gene promoters (Ten et al., 1992), ii) such stimuli can induce complete degradation of p105 by proteasome (Heissmeyer et al., 1999), and iii) the inducible nuclear translocation followed by degradation of nuclear p50 also occurs after cell stimulation (Carmody et al., 2007). Thus, the

details of constitutive p105 and p100 processing remains incompletely understood and are await further investigations.

After more then a decade of studies, it is now appears that the "inducible" processing of p105 does not significantly contribute to cell physiology (Sun and Ley, 2008). Inducible p100 processing, on the other hand, has been intensely investigated following the discovery of the "non-canonical' NF-κB pathway. The outcome of the activation of the non-canonical NF-κB pathway is the nuclear activity of p52-containing NF-κB dimers, which are thought to be generated from p100 heterodimers with other NF-κB subunits, particularly with RelB (Fig. 1.2, middle panel). The non-canonical pathway requires NIK and IKK1 that function downstream of several receptors including lymphotoxin beta receptor (LTβR) (Weih and Caamano, 2003). Interestingly, while NIK is a powerful inducer of processing of the ectopically expressed p100 (Xiao et al., 2001), transient overexpression of NIK in HEK293 cells does not affect the ratio of the endogenous p100 to p52 (A Fusco, personal communication). Thus, it is conceivable that, in context of the non-canonical NF-κB pathway, NIK acts upon newly synthesized p100.

The experiments described in this chapter investigated the mechanisms of p105 and p100 processing. We noted that 20S proteasome can process p105 to p50 in the ubiquitin-independent manner (Moorthy et al., 2006). We followed our observations and compared the accessibility of native and refolded p105 to 20S proteasomal degradation. We found that p105 isolated from cells is resistant to degradation by 20S proteasome compared to the *in vitro* refolded form of p105. Our observation suggests that folding intermediates of p105 is likely to be susceptible for proteolysis by 20S proteasome. We also studied p100 processing in context of activation of non-canonical NF-κB pathway in mouse embryonic fibroblasts. We identified the factor, RelB, which affects the stability of p100 during non-canonical NF-κB signaling downstream of LTβR. In addition, our results showed that RelB also affects the distribution of p100 processed product p52 between the cytoplasmic and nuclear compartments.

4.2. Material and methods

Cell Culture

HEK293T cell line was obtained from Y. Chen (UCSD). Wild type and relb-/-; and nfkb1-/-,nfkb2-/- mouse embryonic fibroblasts (MEF) were obtained from A. Hoffmann (UCSD). Transient transfections of HEK293T cells were assisted with Lipofectamin reagent (Invitrogen) and were performed according to manufacturer protocol. Stable transfections of MEF cells were performed according to retroviral gene transfer protocol (Morgenstern and Land, 1990).

Antibody and other Reagents

Antibodies against RelA (sc372), RelB (sc226), and p105/p50 (sc114) were from Santa Cruz Biotechnology; p105/p50 (#1157); p100/p52 (#1495), and p105-C (#1140) rabbit antisera were a gift from N. Rice (NIH, Bethesda, MD). Anti-LTβR agonistic antibody (clone 4H8) was kindly provided by C. Ware (LJIAI). GFP-specific antibody was from QIAGEN. All other reagents were from commercial suppliers.

Molecular cloning.

Series of mouse p105 deletion mutants were generated by PCR and cloned into pEYFP-C1 vector (Clontech) to express N-terminal YFP fusion proteins in mammalian cells as previously described (Moorthy et al., 2006). To generate YFP-p105-GFP double fusion proteins various YFP-p105 fusion sequences were amplified by PCR and subcloned into pEGFP-N1 vector (Clontech). The cloning of p105 for bacterial expression and plasmid to express FLAG-tagged p105 in HEK293T cells were described in Chapter 3.

p105 purification and refolding

His-tagged p105(1-971) was purified by Ni affinity chromatography (Probond Resin, Invitrogen) under native conditions. The Ni column eluate was treated with 7 M urea and the denatured p105 and p50 polypeptides were separated on a Superdex 200 gel filtration column (Amersham) based on size under denaturing conditions. The p105 fractions were pooled and refolded by dialysis in buffer containing 500mM NaCl; 20mM Tris-HCl, pH7.5; 1mM DTT; 10% glycerol; and 0.1% Triton X-100. The refolded protein was then re-purified by gel filtration chromatography on a Superdex 200 column under native conditions.

Cytoplasmic and Nuclear Fractionation

Cytoplasmic and nuclear fractionation was performed as described in Chapter 2.

Gel Filtration Chromatography of Cytoplasmic Extracts

Analytical gel filtration chromatography of cytoplasmic extracts was performed as described in Chapter 2.

Western Blotting and Immunoprecipitation

YFP and GFP-tagged proteins were detected by the antibody specific for GFP. This antibody recognized both variants of green fluorescent protein, YFP and GFP. p105/p50 and p100/52 were detected using p105/p50 (#1157) and p100/p52 (#1495) rabbit antisera. p105 was also detected by p105/p50 (sc114) antibody specific for p105 and p50 nuclear localization peptide. RelA and RelB were detected using rabbit polyclonal antibodies from Santa Cruz Biotechnology. To immunoprecipitate p105 we used p105-C (#1140) rabbit polyclonal antisera raised against C-terminal peptide of human p105 (0.1µl per reaction). Immunoprecipitation

reactions were supplemented with 50mg/ml of bovine serum albumin to normalize for total protein content and performed according to standard immunoprecipitation protocol (Perr, 2008).

20S proteasome degradation assay

20S proteasome was a gift from M. Rechsteiner and G. Pratt (University of Utah). p105 was immunoprecipitated from whole cell extract or from the solution of refolded p105 (diluted in cell lysis buffer). Immunoprecipitated p105 were mixed with the excess of 20S proteasome in a buffer containing 250mM NaCl; 20mM Tris-HCl, pH7.0; 10mM MgCl2; and 1mM DTT at 37^0C. Samples were removed at various time points and the reaction was stopped by adding SDS-PAGE loading dye and boiling. Proteasome inhibitor MG132 (1mM) (Sigma) was used to control for the specificity of the reactions.

Metabolic Pulse-Chase labeling

HEK293T cells were transfected with vectors expressing FLAG-p105 using Lipofectamin. Growth media was removed 24 hours after transfection and cells were washed twice with labeling media (RPMI 1640 free of methionine and cysteine supplemented with 10% dialyzed fetal calf serum), followed by pulse-labeling with 0.1mCi/mL 35S-Met for 30 minutes. Pulse media was replaced with chase media (labeling media supplemented with 500μg/ml cysteine-HCl and with 100μg/ml methionine) after 30 minutes. Pulsed-labeled cells were lysed in lysis buffer (100mM NaCl; 20mM Tris-HCl, pH8.0; 1% Triton-X100) in the presence of protease and phosphatase inhibitors. 1 mg of protein extract was used to immunoprecipitate FLAG-tagged p105 and p50 using anti-FLAG affinity resin (Sigma). The immunoprecipitated proteins were separated by SDS-PAGE and analyzed by fluorography.

4.3. Results

4.3.1. The site of proteolysis in p105 protein

To determine the site of proteolysis in p105 protein we generated a series of C-terminal deletion mutants of p105. We transfected HEK293T cells with vectors expressing mutant p105 as the N-terminal YFP-fusion proteins and tested if p50 is generated from these precursors (Fig. 4.1). We found that all precursors longer then YFP-p50 undergo processing. Comparing the migration of the precursors and their products on SDS-PAGE gels by western blotting with antibodies specific for YFP tag, we concluded that the processing site appears to be near residue 430 (Fig 4.1). Thereafter, we shall refer to 430 as the site of processing. Our results were consistent with earlier observations made by Blank et al. (Blank et al., 1991). We also observed that the first 244 residues of p105 (that are folded into N-terminal sub-domain of RHD) do not affect the processing of p105 and the p50-like product. p50(~245-430) was generated from every N-terminally truncated p105 mutant that contains processing site (Fig. 4.1B) (Lin and Ghosh, 1996).

4.3.2. p50 is generated by endoproteolysis of p105

We also confirmed that p50 is generated as a result of internal cleavage of p105 polypeptide (Lin and Ghosh, 1996). We overexpressed the p105 fusion proteins in which the p105 fragments were flanked by YFP and GFP. We observe the generation of YFP-p50(~245-430) in all cases where the C-terminus of p105 fragment contained the processing site (Fig. 4.2). Our experiment was designed with the assumption that folded YFP and GFP domains at the termini of the p105 proteins would be protected from “exoproteolysis”.

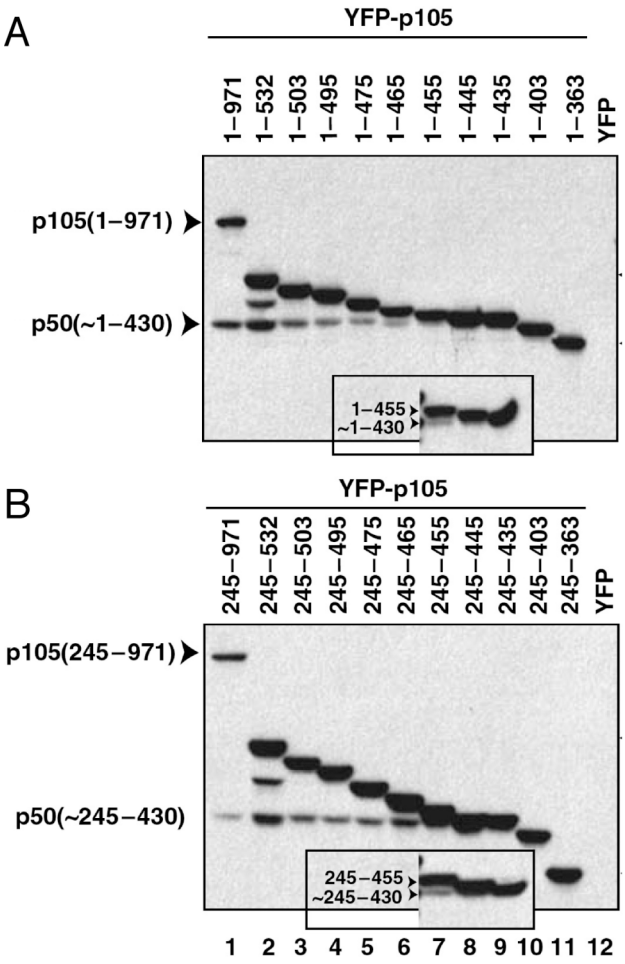

Figure 4.1 p105 processing site corresponds to amino acid ~430

(A) HEK293T cells were transfected with the expression vectors coding for YFP-tagged wild type and C-terminally truncated p105 proteins. Cell lysates were prepared 48 hours after transfection and analyzed by western blotting.

(B) HEK293T cells were transfected with the expression vectors coding for YFP-tagged C-terminally truncated p105 proteins that also lacked the N-terminal domains. Cell lysates were prepared 48 hours after transfection and analyzed by western blotting.

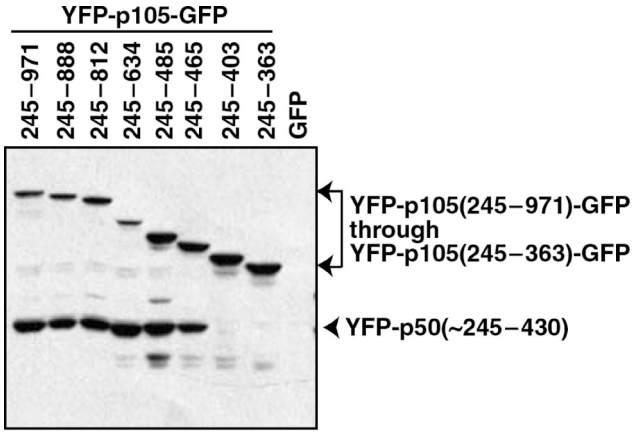

Figure 4.2 Endoproteolytic processing of p105

HEK293T cells were transfected with the expression vectors encoding indicated YFP-p105-GFP double fusion proteins. The precursors and processed products were visualized by western blotting with p50(NLS) antibody.

4.3.3. Isolated endogenous p105 complexes are resistant to 20S proteasome processing *in vitro*

Our *in vitro* experiments showed that 20S proteasome can generate p50 from the refolded recombinant p105 protein as a substrate (Moorthy et al., 2006). This result was interesting because it suggested that i) p105 could be proteolysed in cells by just the catalytic core (20S) of proteasome; ii) p50 could be generated by a post-translational mechanism; iii) ubiquitination is not required for p105 processing.

To further investigate the involvement of 20S proteasome in p105 processing we compared the proteolysis of the refolded p105 and the endogenous p105 complexes purified from HEK293 cells. Both the endogenous and the recombinant p105 was immunoprecipitated (IP) with antibody specific for the C-terminal p105 epitope in lysis buffer and after extensive washes both immunoprecipitates were subjected to 20S proteasome *in vitro*. We observed that the p105 isolated from HEK293 cell was resistant to proteolysis by 20S proteasome while the refolded

p105 degraded in proteasome-depended manner during the course of the reaction (Fig. 4.3A). Due to the limitations of the antibody reagents we could not measure the amounts of p50 by western blotting (p50 band was masked by immunoglobulin heavy chain band, not shown). It has been shown that 20S proteasome can degrade natively unfolded proteins. For example, it has been suggested that the "natively unfolded" p21 protein interact with the aperture of 20S proteasome that allows the entrance if the substrate into the catalytic chamber of 20S proteasome (Chen et al., 2004). We concluded, therefore, that the processing competent p105 might represent the intermediate folding product that could activate 20S proteasome.

During the course of our investigation of the proteolytic stability of p105 we also performed the metabolic pulse-chase experiments in HEK293T cells ectopically expressing FLAG-tagged p105 and analyzed the dynamics of p50 generation in these conditions. Interestingly, we observed the generation of p50 during the early phase of chase period (up to 4 hours) but not at the later time points (Fig. 4.3B). Almost entire pool of radioactively labeled overexpressed p105 remained stable during the whole chase period (12 hours). Only a small fraction of p105 appeared to undergo processing suggesting that a significant pool of p105 became resistant to processing shortly after synthesis.

This experiment also confirmed our earlier observations that the half-life of endogenous p105 is greater then 12 hours (half-life of p105 was obtained from cycloheximide experiments, data not shown). Cycloheximide is an inhibitor of protein biosynthesis and is used in cell culture as an alternative, non-radioactive, method to determine half-life of endogenous proteins.

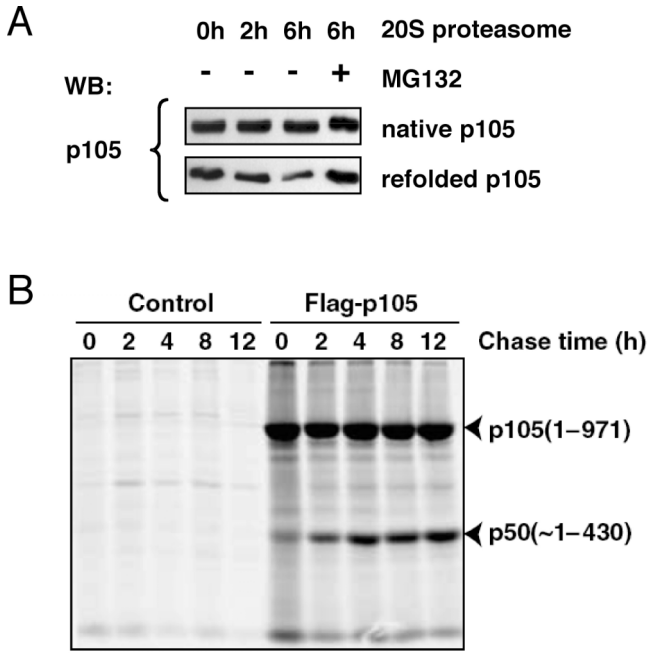

Figure 4.3 Proteolytic stability of endogenous p105

(A) Endogenous p105 (native) or recombinant (refolded) p105 was immunoprecipitated using C-terminal-specific antibody and subjected to proteasomal degradation reaction. MG132 was used to inhibit the activity of proteasome. p105 was detected by western blotting (WB)

(B) HEK293T cells were transfected with the control plasmid or with plasmid encoding FLAG-tagged p105. 24 hours after transfection cells were metabolically labeled with 35S-methionine for 30 min and "chased" for the indicated times. p105 and p50 were precipitated from cell lysates with FLAG peptide specific antibodies conjugated to agarose beads and eluted by boiling in Laemmli sample buffer. Precipitated p105 and p50 were analyzed by SDS-PAGE followed by autoradiography.

4.3.4. RelB stabilizes p100 protein during lymphotoxin beta receptor (LTβR) signaling

p52 NF-κB subunit is generated in response to the non-canonical NF-κB pathway stimuli through the proteasomal processing of p100 precursor. p52-containing NF-κB heterodimers are the nuclear effectors of the non-canonical NF-κB pathway and contribute to the pathway-specific gene regulation (Dejardin et al., 2002).

We analyzed the amounts of p100 and p52 in wild type (wt) and in RelB-deficient (*relb*-/-) mouse embryonic fibroblasts during the course of LTbR stimulation with agonistic antibody (Browning et al., 1995). We observed that in the RelB-deficient cells the inducible p100 processing appears to be enhanced. Moreover, the reconstitution of RelB expression in these cells stabilized the p100 levels during the course of stimulation (Fig. 4.4). A similar effect of RelB on the stability of p100 was observed by Maier and colleagues (Maier et al., 2003). Their experiments showed that reconstituted RelB expression protects p100 from processing to p52, and extends the half-life of p100 in serum-stimulated murine S107 plasmacytoma cells.

We also noted that in the absence of RelB p52 NF-κB subunits re-distributes to low molecular complexes after the reduction of p100 protein levels following LTbR stimulation (Fig. 4.5). This observation points to the inhibitory role of p100 in p52 NF-κB signaling. In the absence of RelB, p100 levels diminish, and less p52 is detected in the high MW complexes post-stimulation in contrast to our previous observation where in the wild type macrophages, treated with LPS, the estimated 50% of "processed" p52 partition into the high MW complexes (Chapter 2).

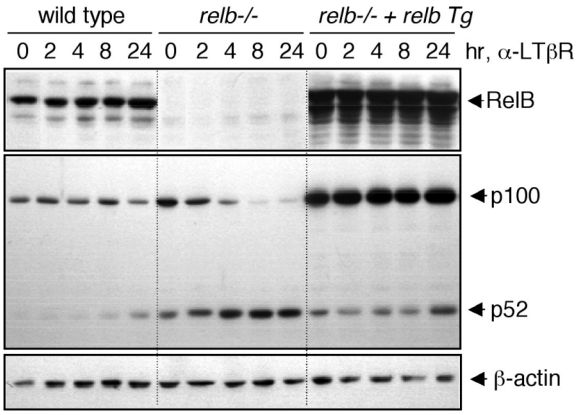

Figure 4.4 RelB stabilizes p100 in fibroblasts stimulated with LTβR agonistic antibody

Wild type, RelB deficient (*relb-/-*), and RelB-reconstituted (*relb-/-* + *relb Tg*) MEF were treated with LTβR agonistic antibody for up to 24 hours. RelB, p100, p52, and β-actin were detected by western blotting in whole cell lysates.

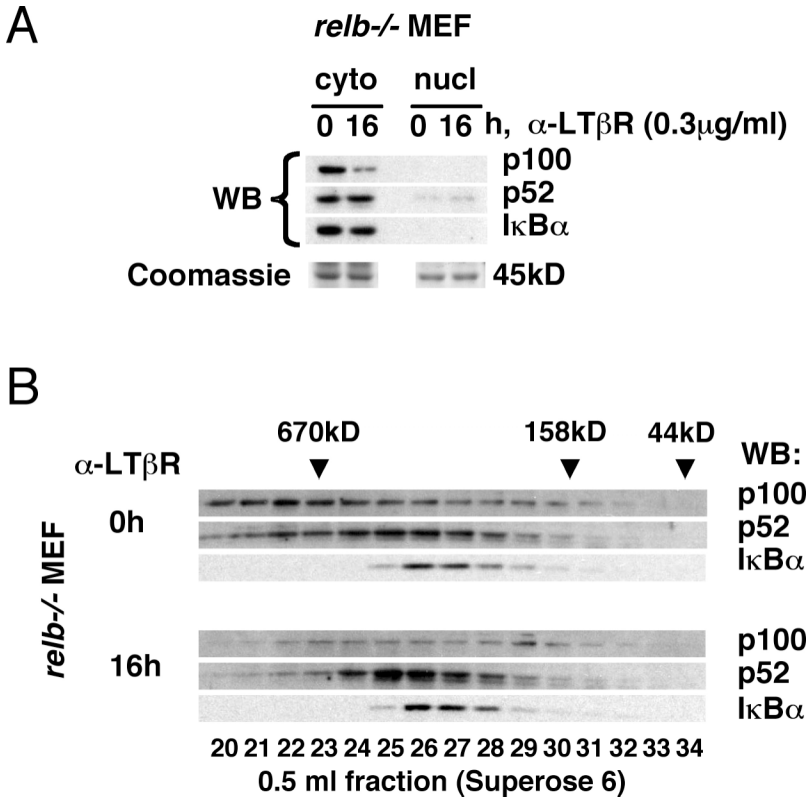

Figure 4.5 p52 re-distributes to low MW complexes in the absence of stable p100

(A) *relb-/-* MEF were stimulated with 0.3μg/ml LTβR agonistic antibody for 16 hours. Cytoplasmic and nuclear extracts were prepared before and after stimulation and analyzed by western blotting (WB) to detect p100, p52, and IκBα.

(B) Cytoplasmic extracts of *relb-/-* MEF (shown in A) were fractionated by gel filtration chromatography and analyzed by WB to detect p100, p52, and IκBα.

4.3.5. Nuclear function of RelB is not required for p100 protein stabilization during LTβR signaling

We aimed to determine if the RelB stabilizing effect on p100 protein during LTβR signaling is due to RelB transcriptional activity or, as we hypothesize, is due to the direct protein-protein interactions of RelB with p100 (Fusco et al., 2008). We mutated the nuclear localization sequence (NLS) of RelB. Mutation of RelB NLS disrupted its nuclear localization thus rendering RelB transcriptionally inactive. Stable expression of such RelB NLS mutant in RelB-deficient mouse embryonic fibroblasts was sufficient to stabilize cytoplasmic p100 level during the course of LTbR stimulation (Fig. 4.6A, "cyto"). We concluded that transcriptional activity of RelB is not required for its protective effect on p100. It appears that the presence of cytoplasmic RelB is sufficient for p100 protein stabilization. In addition, our results also show that mutant RelB that lacks the nuclear localization propensity due to the mutations in the nuclear localization signal region prevents the inducible p52 translocation to the nucleus (Fig. 4.6A, "nucl"). This latter effect of RelB NLS mutant was specific for p52 NF-κB subunit. While p52 NF-κB subunits remained in the cytoplasm, p50 and RelA translocated to the nucleus in stimulus-dependent manner (Fig. 4.6B, "nucl"). These two NF-κB subunits were less affected by the presence of constitutively cytoplasmic RelB. Based on the results described in this section we speculated that p100, p52, and RelB form a subset of high MW NF-κB complexes because i) constitutively cytoplasmic RelB stabilizes p100 protein in *relb-/-* fibroblasts, and ii) this RelB mutant appear to sequester p52 NF-κB subunit in the cytoplasm. The organization and the mechanism of assembly of this type of complexes are remaining to be investigated in detail.

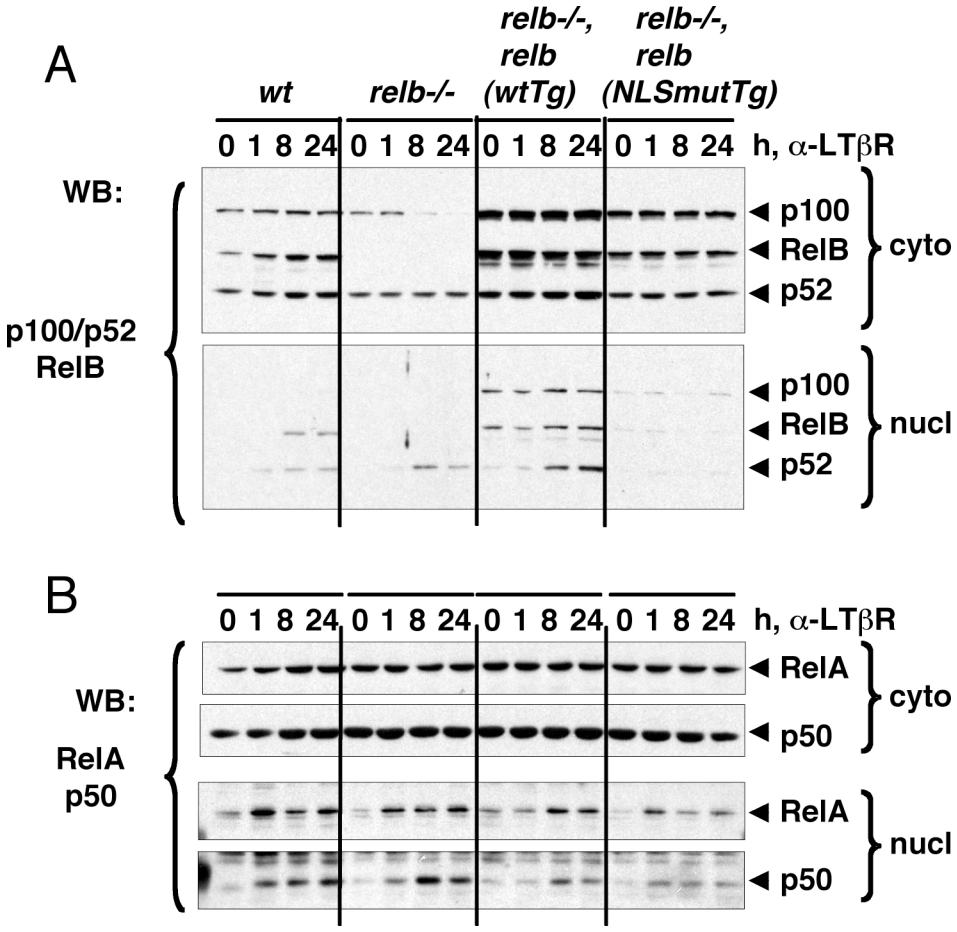

Figure 4.6 Cytoplasmic RelB is sufficient for p100 protein stabilization when LTb receptor is activated

RelB-deficient mouse embryonic fibroblasts (*relb-/-*) were reconstituted with wild type RelB (*relb-/-,relb<wtTg>*) or with RelB nuclear localization mutant (*relb-/-,relb<NLSmutTg>*) by retroviral gene transfer. Cells were treated with 0.3μg/ml of LTβR agonistic antibody for up to 24 hours. Nuclear (nucl) and cytoplasmic (cyto) extracts were prepared and analyzed by western blotting with mixtures of antibodies specific for p100/p52 and RelB (panel A) or RelA and p50 (panel B).

4.4. Discussion

Regulated proteolysis is an important component of p105 and p100 function. Cleavage of p105 and p100 by proteasome with consecutive degradation of their C-terminal fragments gives rises to p50 and p52 NF-κB subunits, respectively. This type of proteolysis is termed "processing". The rate of processing contributes to the balance between the subset of IκB molecules (full-length p105 and p100) and subset of NF-κB subunits (p50 and p52). Thus, the mechanisms of processing continue to be an interest to researchers in NF-κB field.

The studies of the precursor processing were initially focused on the goal of finding the "processing" regions or the intrinsic determinants of processing. Thus, the glycine rich region (GRR), which is located C-terminal to RHD domain and "in front" of the processing site in p105, was found to be sufficient to direct the proteolysis of p105 and other proteins (engineered by molecular cloning to contain p105 GRR) (Lin and Ghosh, 1996). We also showed that sequences C-terminal to p105 processing site are not required initiating processing reaction (Fig. 4.1). There are two interesting mechanistic aspects could be inferred from our observations. First, we noted that YFP-tagged p105 proteins that lack the ANK domain are localized to the nucleus when overexpressed (data not shown). This itself, is not a surprising observation because similar findings were previously reported (Blank et al., 1991; Rice et al., 1992). The processing of these nuclear p105 mutants, however, was evident in our experiments (Fig. 4.1). Thus, our observations imply that either p105 was processed immediately after translation in the cytoplasm (before both the remaining precursors and the products re-localized to the nucleus) or the proteasomal processing could occur in the nucleus. The second interesting observation was that p105 N-terminal fragment, extending only 25 amino acids beyond the site of processing, was also proteolysed to p50. This qualitative observation contradicted the earlier proposed mechanism of co-translational processing of p105 (Lin et al., 1998). This latter mechanism was supported by *in*

vitro studies and suggested that p50 is generated as a result of ribosome pausing on p105 mRNA followed by the recruitment of proteasome that catalyzes the cleavage of nascent p50 polypeptide. The peptide channel in the ribosome, however, covers ~35–50 residues of the growing polypeptide chain. Thus, an extension of 25 residues beyond the processing site is too short to make a nascent peptide accessible for cleavage while the precursor is still bound to the ribosome. We speculate that the intrinsic folding properties of GRR and the p105 processing site facilitate the recruitment of proteasome to p105. Based on our data we exclude the ribosome pausing as an essential factor for p105 processing.

We analyzed the sequence conservation between p105 and p100 proteins based on the alignment of protein sequences encoded by the homologous exons of *NFKB1* and *NFKB2* genes (Fig. 3.12). We found that the GRR is encoded by the conserved exon in both genes. The site of proteolysis, however, is not conserved between the products of two genes. Thus, the mechanism of p105 and p100 processing might be similar due to the conservation of the GRR region, but the rate of processing is different in part due to the differences in the region surrounding the site of proteolysis.

Our pulse-chase experiments with p105 in HEK293 cells indicate that processing of ectopically expressed p105 is restricted to the early time points after radioactive metabolic pulse labeling. We observe that, after the initial proteolysis, p105 remained stable for the extended period of time (Fig 4.3B). This observation points to the requirement for *de novo* synthesis of p105 for proteasomal processing generating p50 NF-κB subunit. Moreover, the comparison of the recombinant p105, which has been refolded *in vitro*, with the endogenous p105, purified from HEK293 cells in the native form (Fig. 4.3B), implies that the folding intermediates of p105 might serve as a substrate for proteasome. We further speculate that the assembly of p105 and p100 complexes protects both proteins from the constitutive processing.

In all, we suggest that activation of NF-κB signaling stimulate p105 and p100 *de novo* protein synthesis and generation of new p50 and p52 subunits by proteolysis of the folding intermediates of p105 and p100. We speculate that activity of NIK and IKK1, the two kinases that are activated by the non-canonical NF-kB pathway and stimulate p100 processing, increase the rate of p100 processing, possibly, by assisting proteasome docking to p100 processing site. Simultaneously, and due to the presence of several binding sites for other NF-κB subunits, p105 and p100 assemble into proteolytically stable NF-κBsomes. Based on the data shown in (Fig. 4.5 and Fig. 4.6) we suggest that p100:p52:RelB – containing high MW complexes may indeed represent such proteolytically stable assembly.

The advantage of our model is that it attempts to connect the p105 and p100 processing with *de novo* protein synthesis, and to the function of p105 and p100 as the inhibitors of NF-κB signaling acting in the negative feedback regulatory loop.

4.5. Chapter 4 acknowledgements

I thank Vivien Wang for performing metabolic pulse-chase experiments, Alexander Hoffmann for *relb-/-* MEF cells; Carl Ware for agonistic antibodies for LTbR1; Rashmi Tawlar and Thomas Ng for molecular cloning and for reconstitution of relb-/- MEF with retroviral vectors encoding wild type and mutant RelB proteins; Nancy Rice and Mary Ernst for p100/p52 rabbit antisera.

I acknowledge the funding from the Graduate Assistance in Areas of National Need (GAANN) program in UCSD in the form of the pre-doctoral fellowship to OVS during 2005/2006.

Figures 4.1, 4.2, and 4.3A in this Chapter 4 are reprinted with permission as it appears in EMBO Journal, 2006. Moorthy, Anu K.; Savinova, Olga V.; Ho, Jessica Q.; Wang, Vivien Y-F.; Vu, Don; Ghosh, Gourisankar. "The 20S proteasome processes NF-κB1 p105 into p50 in a translation independent manner". EMBO; 25(9):1945-56; 2006. The dissertation author was the co-author on this paper.

References

Baeuerle, P.A., and Baltimore, D. (1988). Activation of DNA-binding activity in an apparently cytoplasmic precursor of the NF-kappa B transcription factor. Cell *53*, 211-217.

Banerjee, A., Gugasyan, R., McMahon, M., and Gerondakis, S. (2006). Diverse Toll-like receptors utilize Tpl2 to activate extracellular signal-regulated kinase (ERK) in hemopoietic cells. Proc Natl Acad Sci U S A *103*, 3274-3279.

Basak, S., Kim, H., Kearns, J.D., Tergaonkar, V., O'Dea, E., Werner, S.L., Benedict, C.A., Ware, C.F., Ghosh, G., Verma, I.M., and Hoffmann, A. (2007). A fourth IkappaB protein within the NF-kappaB signaling module. Cell *128*, 369-381.

Beinke, S., and Ley, S.C. (2004). Functions of NF-kappaB1 and NF-kappaB2 in immune cell biology. Biochem J *382*, 393-409.

Belich, M.P., Salmeron, A., Johnston, L.H., and Ley, S.C. (1999). TPL-2 kinase regulates the proteolysis of the NF-kappaB-inhibitory protein NF-kappaB1 p105. Nature *397*, 363-368.

Blank, V., Kourilsky, P., and Israel, A. (1991). Cytoplasmic retention, DNA binding and processing of the NF-kappa B p50 precursor are controlled by a small region in its C-terminus. Embo J *10*, 4159-4167.

Boltz-Nitulescu, G., Wiltschke, C., Holzinger, C., Fellinger, A., Scheiner, O., Gessl, A., and Forster, O. (1987). Differentiation of rat bone marrow cells into macrophages under the influence of mouse L929 cell supernatant. J Leukoc Biol *41*, 83-91.

Bouwmeester, T., Bauch, A., Ruffner, H., Angrand, P.O., Bergamini, G., Croughton, K., Cruciat, C., Eberhard, D., Gagneur, J., Ghidelli, S.*, et al.* (2004). A physical and functional map of the human TNF-alpha/NF-kappa B signal transduction pathway. Nat Cell Biol *6*, 97-105.

Brandman, O., and Meyer, T. (2008). Feedback loops shape cellular signals in space and time. Science *322*, 390-395.

Browning, J.L., Dougas, I., Ngam-ek, A., Bourdon, P.R., Ehrenfels, B.N., Miatkowski, K., Zafari, M., Yampaglia, A.M., Lawton, P., Meier, W., and et al. (1995). Characterization of surface lymphotoxin forms. Use of specific monoclonal antibodies and soluble receptors. J Immunol *154*, 33-46.

Carmody, R.J., Ruan, Q., Palmer, S., Hilliard, B., and Chen, Y.H. (2007). Negative regulation of toll-like receptor signaling by NF-kappaB p50 ubiquitination blockade. Science *317*, 675-678.

Chen, F.E., Kempiak, S., Huang, D.B., Phelps, C., and Ghosh, G. (1999). Construction, expression, purification and functional analysis of recombinant NFkappaB p50/p65 heterodimer. Protein Eng *12*, 423-428.

Chen, X., Chi, Y., Bloecher, A., Aebersold, R., Clurman, B.E., and Roberts, J.M. (2004). N-acetylation and ubiquitin-independent proteasomal degradation of p21(Cip1). Mol Cell *16*, 839-847.

Compton, S.J., and Jones, C.G. (1985). Mechanism of dye response and interference in the Bradford protein assay. Anal Biochem *151*, 369-374.

Dejardin, E., Droin, N.M., Delhase, M., Haas, E., Cao, Y., Makris, C., Li, Z.-W., Karin, M., Ware, C.F., and Green, D.R. (2002). The Lymphotoxin-[beta] Receptor Induces Different Patterns of Gene Expression via Two NF-[kappa]B Pathways. Immunity *17*, 525.

Dobrzanski, P., Ryseck, R.P., and Bravo, R. (1995). Specific inhibition of RelB/p52 transcriptional activity by the C-terminal domain of p100. Oncogene *10*, 1003-1007.

Fan, C.M., and Maniatis, T. (1991). Generation of p50 subunit of NF-kappa B by processing of p105 through an ATP-dependent pathway. Nature *354*, 395-398.

Fan, Z.H., Wang, X.W., Lu, J., Ho, B., and Ding, J.L. (2008). Elucidating the function of an ancient NF-kappaB p100 homologue, CrRelish, in antibacterial defense. Infect Immun *76*, 664-670.

Felsenstein, J. (1989). Mathematics vs. Evolution: Mathematical Evolutionary Theory. Science *246*, 941-942.

Ferrandon, D., Imler, J.L., and Hoffmann, J.A. (2004). Sensing infection in Drosophila: Toll and beyond. Semin Immunol *16*, 43-53.

Freeman, M. (2000). Feedback control of intercellular signalling in development. Nature *408*, 313-319.

Fusco, A.J., Savinova, O.V., Talwar, R., Kearns, J.D., Hoffmann, A., and Ghosh, G. (2008). Stabilization of RelB requires multidomain interactions with p100/p52. J Biol Chem *283*, 12324-12332.

Ghosh, S., Gifford, A.M., Riviere, L.R., Tempst, P., Nolan, G.P., and Baltimore, D. (1990). Cloning of the p50 DNA binding subunit of NF-kappa B: homology to rel and dorsal. Cell *62*, 1019-1029.

Heissmeyer, V., Krappmann, D., Wulczyn, F.G., and Scheidereit, C. (1999). NF-kappaB p105 is a target of IkappaB kinases and controls signal induction of Bcl-3-p50 complexes. Embo J *18*, 4766-4778.

Heusch, M., Lin, L., Geleziunas, R., and Greene, W.C. (1999). The generation of nfkb2 p52: mechanism and efficiency. Oncogene *18*, 6201-6208.

Hoffmann, A., Natoli, G., and Ghosh, G. (2006). Transcriptional regulation via the NF-kappaB signaling module. Oncogene *25*, 6706-6716.

Hohmann, H.P., Remy, R., Scheidereit, C., and van Loon, A.P. (1991). Maintenance of NF-kappa B activity is dependent on protein synthesis and the continuous presence of external stimuli. Mol Cell Biol *11*, 259-266.

Huxford, T., Huang, D.B., Malek, S., and Ghosh, G. (1998). The crystal structure of the IkappaBalpha/NF-kappaB complex reveals mechanisms of NF-kappaB inactivation. Cell *95*, 759-770.

Karin, M., and Lin, A. (2002). NF-kappaB at the crossroads of life and death. Nat Immunol *3*, 221-227.

Karlebach, G., and Shamir, R. (2008). Modelling and analysis of gene regulatory networks. Nat Rev Mol Cell Biol *9*, 770-780.

Kawai, T., and Akira, S. (2007). Signaling to NF-kappaB by Toll-like receptors. Trends Mol Med *13*, 460-469.

Kieran, M., Blank, V., Logeat, F., Vandekerckhove, J., Lottspeich, F., Le Bail, O., Urban, M.B., Kourilsky, P., Baeuerle, P.A., and Israel, A. (1990). The DNA binding subunit of NF-kappa B is identical to factor KBF1 and homologous to the rel oncogene product. Cell *62*, 1007-1018.

Lalli, E., and Sassone-Corsi, P. (1994). Signal transduction and gene regulation: the nuclear response to cAMP. J Biol Chem *269*, 17359-17362.

Legarda-Addison, D., and Ting, A.T. (2007). Negative regulation of TCR signaling by NF-kappaB2/p100. J Immunol *178*, 7767-7778.

Lin, L., DeMartino, G.N., and Greene, W.C. (1998). Cotranslational biogenesis of NF-kappaB p50 by the 26S proteasome. Cell *92*, 819-828.

Lin, L., and Ghosh, S. (1996). A glycine-rich region in NF-kappaB p105 functions as a processing signal for the generation of the p50 subunit. Mol Cell Biol *16*, 2248-2254.

Liou, H.C., Nolan, G.P., Ghosh, S., Fujita, T., and Baltimore, D. (1992). The NF-kappa B p50 precursor, p105, contains an internal I kappa B-like inhibitor that preferentially inhibits p50. Embo J *11*, 3003-3009.

Maier, H.J., Marienfeld, R., Wirth, T., and Baumann, B. (2003). Critical role of RelB serine 368 for dimerization and p100 stabilization. J Biol Chem *278*, 39242-39250.

Mercurio, F., Didonato, J., Rosette, C., and Karin, M. (1992). Molecular cloning and characterization of a novel Rel/NF-kappa B family member displaying structural and functional homology to NF-kappa B p50/p105. DNA Cell Biol *11*, 523-537.

Mercurio, F., DiDonato, J.A., Rosette, C., and Karin, M. (1993). p105 and p98 precursor proteins play an active role in NF-kappa B-mediated signal transduction. Genes Dev *7*, 705-718.

Michelsen, K.S., Wong, M.H., Shah, P.K., Zhang, W., Yano, J., Doherty, T.M., Akira, S., Rajavashisth, T.B., and Arditi, M. (2004). Lack of Toll-like receptor 4 or myeloid differentiation factor 88 reduces atherosclerosis and alters plaque phenotype in mice deficient in apolipoprotein E. Proc Natl Acad Sci U S A *101*, 10679-10684.

Moorthy, A.K., Savinova, O.V., Ho, J.Q., Wang, V.Y., Vu, D., and Ghosh, G. (2006). The 20S proteasome processes NF-kappaB1 p105 into p50 in a translation-independent manner. Embo J *25*, 1945-1956.

Mordmuller, B., Krappmann, D., Esen, M., Wegener, E., and Scheidereit, C. (2003). Lymphotoxin and lipopolysaccharide induce NF-kappaB-p52 generation by a co-translational mechanism. EMBO Rep *4*, 82-87.

Morgenstern, J.P., and Land, H. (1990). Advanced mammalian gene transfer: high titre retroviral vectors with multiple drug selection markers and a complementary helper-free packaging cell line. Nucleic Acids Res *18*, 3587-3596.

Natoli, G., and Chiocca, S. (2008). Nuclear ubiquitin ligases, NF-kappaB degradation, and the control of inflammation. Sci Signal *1*, pe1.

Orian, A., Gonen, H., Bercovich, B., Fajerman, I., Eytan, E., Israel, A., Mercurio, F., Iwai, K., Schwartz, A.L., and Ciechanover, A. (2000). SCF(beta)(-TrCP) ubiquitin ligase-mediated processing of NF-kappaB p105 requires phosphorylation of its C-terminus by IkappaB kinase. Embo J *19*, 2580-2591.

Palombella, V.J., Rando, O.J., Goldberg, A.L., and Maniatis, T. (1994). The ubiquitin-proteasome pathway is required for processing the NF-kappa B1 precursor protein and the activation of NF-kappa B. Cell *78*, 773-785.

Pan, Q., Kravchenko, V., Katz, A., Huang, S., Ii, M., Mathison, J.C., Kobayashi, K., Flavell, R.A., Schreiber, R.D., Goeddel, D., and Ulevitch, R.J. (2006). NF-kappa B-inducing kinase regulates selected gene expression in the Nod2 signaling pathway. Infect Immun *74*, 2121-2127.

Perr, B.K.a.M. (2008). Isolation of proteins and protein complexes by immunoprecipitation, Vol 1 (Totowa, NJ: Human Press).

Raschke, W.C., Baird, S., Ralph, P., and Nakoinz, I. (1978). Functional macrophage cell lines transformed by Abelson leukemia virus. Cell *15*, 261-267.

Rice, N.R., MacKichan, M.L., and Israel, A. (1992). The precursor of NF-kappa B p50 has I kappa B-like functions. Cell *71*, 243-253.

Salmeron, A., Janzen, J., Soneji, Y., Bump, N., Kamens, J., Allen, H., and Ley, S.C. (2001). Direct phosphorylation of NF-kappaB1 p105 by the IkappaB kinase complex on serine 927 is essential for signal-induced p105 proteolysis. J Biol Chem *276*, 22215-22222.

Scheidereit, C. (2006). IkappaB kinase complexes: gateways to NF-kappaB activation and transcription. Oncogene *25*, 6685-6705.

Scott, M.L., Fujita, T., Liou, H.C., Nolan, G.P., and Baltimore, D. (1993). The p65 subunit of NF-kappa B regulates I kappa B by two distinct mechanisms. Genes Dev *7*, 1266-1276.

Souvannavong, V., Saidji, N., and Chaby, R. (2007). Lipopolysaccharide from Salmonella enterica activates NF-kappaB through both classical and alternative pathways in primary B Lymphocytes. Infect Immun *75*, 4998-5003.

Sun, S.C., and Ley, S.C. (2008). New insights into NF-kappaB regulation and function. Trends Immunol *29*, 469-478.

Ten, R.M., Paya, C.V., Israel, N., Le Bail, O., Mattei, M.G., Virelizier, J.L., Kourilsky, P., and Israel, A. (1992). The characterization of the promoter of the gene encoding the p50 subunit of NF-kappa B indicates that it participates in its own regulation. EMBO J *11*, 195-203.

Tergaonkar, V., Correa, R.G., Ikawa, M., and Verma, I.M. (2005). Distinct roles of IkappaB proteins in regulating constitutive NF-kappaB activity. Nat Cell Biol *7*, 921-923.

Thompson, J.D., Higgins, D.G., and Gibson, T.J. (1994). CLUSTAL W: improving the sensitivity of progressive multiple sequence alignment through sequence weighting, position-specific gap penalties and weight matrix choice. Nucleic Acids Res *22*, 4673-4680.

Tsuchiya, S., Kobayashi, Y., Goto, Y., Okumura, H., Nakae, S., Konno, T., and Tada, K. (1982). Induction of maturation in cultured human monocytic leukemia cells by a phorbol diester. Cancer Res *42*, 1530-1536.

Tsuchiya, S., Yamabe, M., Yamaguchi, Y., Kobayashi, Y., Konno, T., and Tada, K. (1980). Establishment and characterization of a human acute monocytic leukemia cell line (THP-1). Int J Cancer *26*, 171-176.

Weih, F., and Caamano, J. (2003). Regulation of secondary lymphoid organ development by the nuclear factor-kappaB signal transduction pathway. Immunol Rev *195*, 91-105.

Xiao, G., Harhaj, E.W., and Sun, S.C. (2001). NF-kappaB-inducing kinase regulates the processing of NF-kappaB2 p100. Mol Cell *7*, 401-409.

Yan, Z.Q., and Hansson, G.K. (2007). Innate immunity, macrophage activation, and atherosclerosis. Immunol Rev *219*, 187-203.